ANALYTICS FOR SUSTAINABLE AND RETAIL OPERATIONS

A Dissertation
Presented to
The Academic Faculty

By

Yasaman Mohammadshahi

In Partial Fulfillment
of the Requirements for the Degree
Doctor of Philosophy in the
H. Milton Stewart School of Industrial and Systems Engineering (ISyE)

Georgia Institute of Technology

August 2020

ANALYTICS FOR SUSTAINABLE AND RETAIL OPERATIONS

Approved by:

Dr. L.Beril Toktay, Advisor
Scheller College of Business
Georgia Institute of Technology

Dr. Pinar Keskinocak, Advisor
H. Milton Stewart School of Industrial and Systems Engineering
Georgia Institute of Technology

Dr. He Wang, Advisor
H. Milton Stewart School of Industrial and Systems Engineering
Georgia Institute of Technology

Dr. David Goldsman
H. Milton Stewart School of Industrial and Systems Engineering
Georgia Institute of Technology

Dr. Kris Ferreira
Harvard Business School
Harvard University

Date Approved: July 3, 2020

"*What you seek is seeking you.*"

Rumi

To my beloved parents, Fereshteh and Mohammad, for their unconditional love and support.

ACKNOWLEDGMENTS

First and foremost, I would like to express my sincere gratitude to my advisors, Dr. Beril Toktay and Dr. Pinar Keskinocak, for their guidance and financial support during the past three years. They encouraged me to take the lead and define my own research path; their flexibility enabled me to pursue the research area that I am truly excited about. Being a female PhD student, they have always been my role models as pioneering women in academia.

I am also deeply thankful to Dr. Kris Ferreira and Dr. He Wang who closely guided my PhD research. Kris advised me on my first project in operations management (Chapter 3), and patiently helped me with the transition from pure statistics to operations management analytics. Working under her supervision for two years was a priceless experience. In the last year, I had the honor of working with He. I thank him for kindly accepting to join the Chapter 2 project when I reached out to him. I tremendously learned from his precious advice and brilliant ideas. I also thank Dr. David Goldsman for serving on my dissertation committee and offering memorable classes in statistics.

Chapter 2 was done in collaboration with the Environmental Protection Agency. First, I would like to thank the Research and Development (R&D) office and Enforcement and Compliance Assurance (DECA) team of the EPA headquarter; they helped me navigate through the data-driven sustainability research and connected me with the experts. I am also very grateful to the EPA Region 2 Clean Air Act (CAA) data management team. Doing an internship in their group gave me an invaluable opportunity to gain field knowledge and work on real-world problems. I am especially thankful to Daniel Teitelbaum, Stephanie

Wilson, and Nancy Rutherford for their continuous support. For chapter 3, I also appreciate the excellent advice and guidance of Dr. Gurhan Kok.

Throughout my life, I have been very fortunate to have amazing friends. I would especially like to thank Mahshid Fazel and Sara Kaboudvand. Mahshid has always inspired me by her perseverance and integrity since the initial days of high school that we met. She taught me to be deaf to negative thoughts and stronger than any obstacle that I face while pursuing my dreams. I also profoundly thank Sara for being an incredibly kind, caring, and supportive friend and officemate. I am forever indebted to her for being on my side and taking care of me in the hardest and most stressful days of this journey.

A very special thanks goes to my fantastic friend Jan Vlachy. I learned from Jan in diverse aspects, from data science and optimization to history and literature. He has been a great mentor for me, and his comments dramatically enhanced my research. I also wholeheartedly thank my friend and former officemate Geet Lahoti. We have taken classes and studied for the comprehensive exams together. He has always been there for me in all the ups and downs of graduate life.

I would like to thank my dear friends Samaneh Ebrahimi, Satya Malladi, Chitta Ranjan, and Geet in the "ISyE big potatoes gang". Our Hiking days, game nights, and Indian-Iranian foods and parties are among my sweetest memories. I am also thankful to Amin Gholami, Moussa Hodjat-Shamami, and Sajad Khodadadian; I genuinely enjoyed the afternoon teas, movie nights, exploring Atlanta restaurants, and our recent quarantine Face Time catch-ups. To the rest of my friends in ISyE, Atlanta, and Tehran, thank you all!

Last but certainly not least, I am extremely grateful to my parents, grandparents, and aunt for their immeasurable love and support. Despite being thousands of miles away, you have been in my heart in every moment of the past six years. My exceptional thanks goes to Nogol for being a wonderful sister. My fondest wish is to reunite and hug each of you after this long separation.

TABLE OF CONTENTS

Acknowledgments v

List of Tables xi

List of Figures xiii

Summary xv

Chapter 1: Introduction and Background 1

1.1 Priority-Based Environmental Inspection Strategy 1

1.1.1 Problem Definition 3

1.1.2 Statement of Contributions 3

1.2 Multiproduct Demand Prediction and Price Optimization using Neural Networks 4

1.2.1 Problem Definition 4

1.2.2 Statement of Contributions 5

Chapter 2: Priority-Based Environmental Inspection Strategy 7

2.1 Introduction 7

2.1.1 Contributions to Literature and Practice 9

2.2 Model 11

2.2.1 Facilities' Compliance State Evolution 11

2.2.2 Regulator's Observable Markov Chain and the Restless Multiarmed Bandit Formulation 14

2.3 An Index-Based Inspection Policy 17

2.3.1 Definitions of Indexability and Whittle's Index 18

2.3.2 Proof of the Indexability Condition 19

2.3.3 Whittle's Index Policy for Multiple Facilities 21

2.4 Extensions 22

2.4.1 Inspections with Heterogeneous Resource Requirements 22

2.4.2 Disaster Occurrence 23

2.5 Model Calibration 28

2.5.1 Data Description 28

2.5.2 Characterizing the Current Practice 31

2.5.3 Characterizing the Compliance and Restoration Transition Probabilities 31

2.6 Simulation 38

2.6.1 Scenarios for Inspection Capacity Allocation 39

2.6.2 Inspection Policies 40

2.6.3 Simulation Results and Policy Implications 41

2.7 Policy Implications and Managerial Insight 46

2.8 Conclusion 48

Chapter 3: Multiproduct Demand Prediction and Price Optimization Using Neural Networks 49

3.1 Introduction 49

3.2 Price Elasticity Definition 50
3.2.1 Focal Product Elasticity 50
3.2.2 Substitutable Product Cross-Price Elasticity 50
3.2.3 Competitor's Product Cross-Price Elasticity 51
3.3 Contributions to Literature and Practice 51
3.4 Demand Prediction Model 53
3.4.1 Our Partner Retailer and its Current Pricing Strategy 53
3.4.2 Data Aggregation Level & Demand Prediction Components 54
3.4.3 Products' Similarity Analysis 57
3.4.4 Linear Regression Model 58
3.4.5 An Alternative Demand Prediction Model: Structure-Imposed Neural Network 59
3.5 Price Optimization 65
3.5.1 Mathematical Representation of the structure-imposed Neural Network 66
3.5.2 Price Optimization Tool 66
3.5.3 Impact of the Proposed Pricing Decision Tool on the Retailer Revenue 71
3.6 Conclusion 72

Chapter 4: Concluding Remarks 73

Chapter A: Proofs of the Chapter 2 77

Chapter B: Detailed Steps of Chapter 2 Data Processing 82

B.1 Facilities Information 82

B.2 Inspection and Enforcement History 83

B.2.1 Regular Inspections. 83

B.2.2 Restoration Inspections. 84

References 91

LIST OF TABLES

2.1 Facilities' characteristics and their number of levels. 30

2.2 Conducted Regular Inspections Statistics for EPA Region 2 during 2002-2016. 31

2.3 Average restoration time statistics for EPA Region 2 facilities during 2002-2016. 33

2.4 Average past paid penalty as the measure of environmental harm for EPA Region 2 facilities during 2002-2016. 36

2.5 Estimated parameters for the EPA Region 2 facilities (Ward's minimum variance linkage agglomerative HCA). 37

2.6 Performance comparison of the inspection policies under different capacity allocation scenarios. 41

2.7 Performance comparison of inspection policies compared to the EPA 2/5 policy under different capacities-1/0.8 workload scenario. 45

2.8 Capacity allocation among clusters under different inspection policies-1/0.8 workload. 47

3.1 Overview of the data provided by the retailer. 54

3.2 Estimated elasticities for TVs bestsellers by linear regression (elasticities are recorded for 10% increase in the corresponding prices). 59

3.3 Estimated elasticities for TVs bestsellers by a structure-imposed neural network (elasticities are recorded for 10% increase in the corresponding prices). 63

3.4 Comparison of the linear regression and structured neural network in elasticity estimation and prediction accuracy (average sales is 7). 64

3.5 Prediction accuracy of various prediction models (average sales:7). 64

B.1 Data sources. 85

LIST OF FIGURES

1.1 Environmental Protection Agency regions.[1] 2

1.2 Schematic structure of a neural network. 5

2.1 Hidden Markov chain transition probabilities of facility n when it is not inspected (NI) in a period. 13

2.2 Hidden Markov chain transition probabilities of facility n if it is inspected (I) in a period. 14

2.3 Observable Markov chain transition probabilities of facility n in a period with no inspection (NI). 15

2.4 Observable Markov chain transition probabilities of facility n in a period with inspection (I). 16

2.5 Observable Markov chain transition probabilities of facility n in a period with inspection (I). 17

2.6 Plots of the mean and standard deviation over the mean of the time intervals between two consecutive Whittle's index suggested inspections for each facility ($N = 50$, $M = 10$, and $T = 20$). 22

2.7 Hidden Markov chain transition probabilities of facility n if it is not inspected (NI) in a period (Disaster Included). 24

2.8 Hidden Markov chain transition probabilities of facility n if it is inspected (I) in a period (Disaster Included). 24

2.9 Observable Markov chain transition probabilities of facility n in a period with no inspection (NI) (Disaster Included). 25

2.10 Observable Markov chain transition probabilities of facility n in a period with inspection (I) (Disaster Included). 26

2.11 Observable Markov chain transition probabilities of facility n in a period with inspection (I) (Disaster Included). 26

2.12 Plots of the within clusters sum of squares versus number of clusters (elbow method) for Ward's minimum variance linkage agglomerative hierarchical clustering of the major and SMI facilities. 34

2.13 Two states transition probabilities of facility n if it is not inspected (NI) in a period. 35

2.14 Percentage and average interval of the inspections assigned to each cluster of facilities-1/1 workload scenario. 42

2.15 Percentage and average interval of the inspections assigned to each cluster of facilities-1/0.8 workload scenario. 43

2.16 Percentage and average interval of the inspections assigned to each cluster of facilities-separate capacity per facility size scenario. 44

3.1 General structure of neural networks. 61

3.2 Schematic structure of the proposed neural network. 62

3.3 Structure of the proposed neural network implemented in MATLAB. 63

3.4 Plots of the z-score of the focal product price versus its own revenue function-single product pricing scenario. 70

SUMMARY

This dissertation focuses on two applications of analytics in sustainable and retail operations.

In chapter 2, we design a priority-based inspection strategy for the Environmental Protection Agency (EPA) Region 2. Government regulators such as the U.S. EPA are obligated to inspect facilities regularly to ensure compliance with environmental laws and requirements. Faced with limited budget and resources, regulators can only inspect a small fraction of facilities within a specific time frame. We propose a new inspection strategy that can help environmental regulators prioritize facilities to be inspected under a limited budget. We formulate the problem as a restless multiarmed bandit model and develop an index-based inspection policy. We also demonstrate how to extend the model to incorporate heterogeneous inspection costs and the possibility of environmental disaster. Simulations using data from EPA Region 2 indicate the benefits of our proposed index-based compliance monitoring strategy over other benchmark policies used in academic literature and practice in reducing the harm to the environment and public health.

In chapter 3, we partner with a consumer electronics retailer, and show how incorporating substitution and competition effects, two integral components of today's competitive markets, enhance the accuracy of the demand prediction models. The complicated relationship between the demand of the focal product and the substitutes' prices makes linear models incapable of estimating the cross-price elasticities. We suggest a structure-imposed neural network and demonstrate how it can be utilized in multiproduct pricing decision tools. Our imposed structure mitigates the practical concerns around the interpretability of the neural networks, which has hindered their adoption in revenue management.

CHAPTER 1
INTRODUCTION AND BACKGROUND

The vast proliferation of data has significantly transformed managerial decision making in recent years. Data has enabled managers to comprehend the dynamics of their organizations in more depth, shifting operational decision making from the traditional "going with gut" approach to more informed "analytical" procedure.

Using data has brought enormous values to both nonprofit and for-profit organizations. Data-enabled processes increase the productivity and reduce the inefficiency in both types of organizations [49].

In for-profit organizations such as retailers, data-driven operations have brought tremendous monetary profits to the companies. Recent research demonstrates that companies that extensively use customer analytics are 23 times more likely to acquire customers, enjoy nine times more customer loyalty, and around 19 times more customer profitability. Aside from the organizations, their customers also significantly benefit from their practice of analytics. For example, these companies deliver 15 times more value to the customers and have around six times more customer satisfaction [48].

In this dissertation, we show how analytics can stand at the forefront of transformational efforts in not-for-profit and for-profit operations. We provide a more in-depth overview of each chapter and their contributions next.

1.1 Priority-Based Environmental Inspection Strategy

In chapter 2, we present an application of analytical models in sustainable operations. Environmental Protection Agency (EPA) has ten regional offices in the United States, with each office being responsible for a few states (Figure 1.1). One of the major responsibilities of the EPA in each region is assuring facilities abidance by the environmental laws and regulations,

including Clean Air Act (CAA), Clean Water Act (CWA), Resource Conservation and Recovery Act (RCRA).

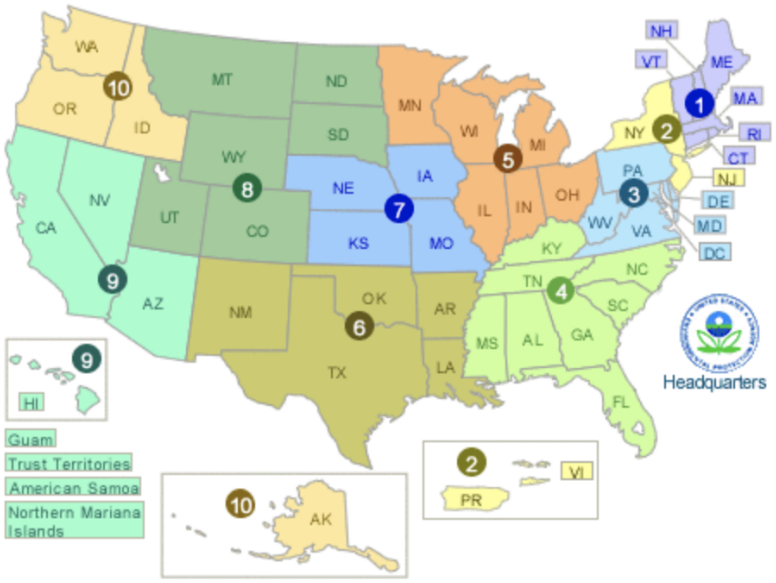

Figure 1.1: Environmental Protection Agency regions.[1]

This chapter reflects our collaboration with the CAA data management team within the Department of Environmental Compliance Assurance (DECA) of the Environmental Protection Agency (EPA) Region 2 office. This office covers facilities within the states of New York, New Jersey, Puerto Rico and the U.S. Virgin Islands.

CAA initially passed in 1963 and was significantly amended in the 1970s and 1990s [20]. Since then, it has been highly beneficial in protecting the environment and public health, and consequently reducing the economic burden associated with air pollution. From an environmental perspective, the CAA is estimated to have contributed to a 74% decrease in the combined emission of six major pollutants (particulate matter 2.5, particulate matter 10, sulfur dioxide, nitrogen oxides, volatile organic compounds and lead) between 1970 and 2018 [25], while the U.S. gross domestic product increased more than 200% in the same period. From a public health perspective, CAA is estimated to have prevented over 160,000

[1] https://www.epa.gov/aboutepa/visiting-regional-office

early deaths, 130,0000 heart diseases, and 1.7 million asthma exacerbations in 2010. These numbers are expected to be as high as 230,000, 200,000, and 2.4 million respectively for 2020 [21].

1.1.1 Problem Definition

Assuring compliance with CAA regulations takes place through the EPA and its analogous states inspections. Budget and time constraints significantly limit the number of inspections that can be performed in each period. To tackle the resource limitation problem, EPA recommends a cyclic policy with intervals depending on facilities' emission size [24]. Specifically, EPA divides facilities into three main categories of major, synthetic minor (SMI) and minor facilities with respect to their emission level, and suggests every two and five years intervals for the inspection of major and SMI facilities.

EPA also allows designing a facility-by-facility inspection strategy that takes the facilities' features and inspection history into account [24]. We develop an individualized inspection strategy for the Region 2 facilities and show the advantages of our proposed policy over different benchmarks.

1.1.2 Statement of Contributions

Our main contributions in chapter 2 are as follows:

- We model the EPA facility selection problem as a restless multiarmed bandit, in which selecting a facility for inspection is similar to pulling an arm in the multiarmed bandit setting. We prove our problem's indexability and show that our proposed policy (under a fixed inspection capacity) is asymptotically optimal as the number of facilities goes to infinity.

- Our model differentiates between the high priority violations and regular (low priority) violations; it also considers the time that facilities require to restore from any violations.

Additionally, it takes into account the potential harm (relative to the other facilities) that a facility can impose on the environment.

- We estimate our model's parameters based on the comprehensive data set of the EPA Region 2 facilities' inspections. We use a clustering approach to increase the estimation robustness.

- We conduct extensive simulations to investigate the performance of our proposed policy over the current EPA practice and other common inspection strategies. We also study the performance of our policy under various capacities and inspection capacity allocation scenarios.

1.2 Multiproduct Demand Prediction and Price Optimization using Neural Networks

In chapter 3, we switch gear to study an application of deep learning in designing pricing decision tools. Most of the pricing decision tools are designed using linear demand prediction models such as linear, log-linear, constant elasticity, and logit demand functions [62]. Linear demand prediction models have shown efficiency in single product pricing problems, but in practice, usually more than just one product's price is changed at a time. Thus, retailers must understand how changing the price of a product impacts the demand of the other products in the category. In addition to the products within the same category, many of the products are offered by different retailers. In recent years, many of the major retailers post their products' prices online regularly, and costumers can compare the prices before making a purchase. Consequently, retailers also need to incorporate the competition effect in their pricing tools.

1.2.1 Problem Definition

The goal of chapter 3 is addressing the substitution and competition effects in designing pricing decision tools. The impact of the substitutable and competitors' products' prices on

demand of the main product can be complicated for the linear models to account for.

We show how neural networks can be helpful in measuring the substitutable and competitor cross-price elasticities. Neural networks are powerful and widely applied prediction tools capable of capturing nonlinear and complicated relationships. Figure 1.2 depicts a schematic structure of a neural network. Their structures consist of three main components: input layers, one or more hidden layer(s), and output layer. Each of the layers has one or more nodes. There are activation functions (linear or nonlinear) in the hidden layer nodes, which are gates between the node inputs and the output going to the next layer.

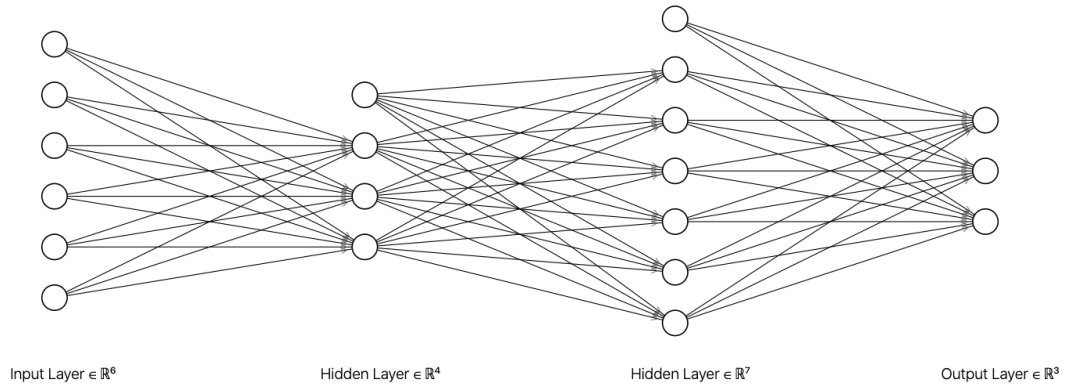

Figure 1.2: Schematic structure of a neural network.

The structures of the neural networks tend to be complicated and black-box. It is generally impossible to state the relationship between the inputs and outputs or address the causal effects in the networks. As a result, neural networks are unsuitable for settings such as pricing in which the relationship of the output (revenue or demand) with input (price) needs to be captured.

1.2.2 Statement of Contributions

In chapter 3, we propose a flexible yet interpretable structure-imposed neural network for multiproduct demand prediction and provide its subsequent optimization technique. The main contributions are listed below:

- We show how neural networks can predict the demand and estimate the substitutable and competitor cross-price elasticities by proposing a structure-imposed neural network. Our suggested network is able to account for the complicated relationship between the substitutable and competitor prices with the demand of the focal products while having mathematical and managerial explanations. Our work is particularly novel in the revenue management literature since the neural networks' black-box nature impedes their application in pricing.

- We write the detailed mathematical formulation of the structure-imposed neural network demand (revenue) function and provide the relationship between the focal, substitutable, and competitors' prices with the demand (and revenue) of each product. Additionally, we provide an optimization approach to solve the subsequent multiproduct pricing optimization problem.

CHAPTER 2

PRIORITY-BASED ENVIRONMENTAL INSPECTION STRATEGY

2.1 Introduction

Environmental pollution, and in particular, air pollution, results in severe adverse health outcomes globally. In 2016, ambient air pollution accounted for 7.6% of all the deaths in the world according to the World Health Organization [69]. In the United States, 516 Disability Adjusted Life Years (DALY) and 24 deaths per 100,000 people were attributed to ambient air pollution in the same year [69].

The Clean Air Act (CAA) is the primary federal regulation aimed at controlling air quality in the United States, and covers combined emissions of six major pollutants (particulate matter 2.5, particulate matter 10, sulfur dioxide, nitrogen oxides, volatile organic compounds and lead) [20]. Compliance with the CAA translates into significant public health gains, measured by the prevention of early deaths, heart disease and asthma [25].

Ensuring facilities' CAA compliance is the responsibility of the Office of Enforcement and Compliance Assurance (OECA) within the Environmental Protection Agency (EPA). To foster facilities' compliance with CAA, EPA partners with states and tribes to inspect facilities (such as chemical plants, power plants, manufacturing operations, and gas stations) and assess their conformity with all the applicable rules. In case of violations, OECA is further required to execute enforcement actions and compel the violating facilities to achieve compliance.

Despite the critical role of inspections in assuring environmental protection and public health, EPA and its partners are only able to inspect a small portion of the potential polluters every year due to resource limitations. The recent drastic decrease in EPA OECA's budget results in even fewer inspections than before; the United State's proposed budget in March

2017 cut the funds of OECA by 24%, and the delegated inspection fund from EPA to states also decreased from $1.1 billion to $597 million [16]. This highlights the importance of an effective Compliance Monitoring Strategy (CMS) to help OCEA identify the facilities that are most likely to harm the environment and public health, and prioritize them for inspection.

The EPA's current CAA Compliance Monitoring Strategy applies a simple "cyclic" rule: facilities are inspected at fixed time intervals whose length depends on their emission quantity. More specifically, facilities are divided into three main categories, Major, Synthetic Minor (SMI), and Minor, with respect to their emission levels. The recommended inspection frequency is every two and five years for major and SMI facilities, respectively; there is no specific guidance for minor facility inspection frequency. For example, in EPA Region 2 (covering New York, New Jersey, Puerto Rico and the U.S. Virgin Islands), there are currently 19,374 facilities, among which 4.30% are major, 22.31% are SMI, and 73.39% are minor.

The new Compliance Monitoring Strategy issued in October 2016, known as the flexible CAA CMS, allows the regulators to *individualize* the inspection plans, and develop alternative compliance monitoring strategies on a facility-by-facility basis. The Alternative Compliance Monitoring Strategy (ACMS) recommends taking into account the facility's characteristics, including the facility's compliance history, its location, its potential environmental impact, etc. in determining how frequently to inspect it [24].

The academic literature, to the best of our knowledge, has not considered developing an individualized inspection targeting strategy in the presence of a tight budget constraint. In this chapter, motivated by the CAA program, we design an Individualized Compliance Monitoring Strategy that meets EPA requirements. We demonstrate the advantages of our recommended policy via simulation using data from EPA Region 2 on facilities' features and compliance histories.

Our methodology is not only applicable to the CAA program, but also other programs of

the OECA such as Resource Conservation and Recovery Act (RCRA) and Clean Water Act (CWA), and more broadly, inspection targeting strategies for environmental compliance.

2.1.1 Contributions to Literature and Practice

Our model considers a regulator who selects a set of facilities to inspect in each period. The regulator has a resource restriction that limits the number of inspections that can be conducted per period. The regulator's objective is to minimize the long-run average harm to the environment from noncompliance.

We formulate the facility selection process as a restless multiarmed bandit (RMAB) problem [68] in which each facility represents an arm and choosing a facility can be interpreted as pulling the arm. We develop an *index policy* that determines the regulator's inspection priorities in each period. The indices are computed according to the regulator's belief regarding facilities' probabilities of noncompliance, which depend on facilities' attributes. These attributes contain both static and dynamic features of the facility such as location, type of industry, emission types, demographic characteristics, and compliance history data (inspection and enforcement history). This information is exogenous and available to the regulator prior to its decision making in every period.

There are several operations management papers that consider restless bandits and index policies for resource allocation. [36] utilize a restless multiarmed bandit model to design a maintenance policy for multiple machines with limited repairmen. [14] propose an index policy to tackle the assortment optimization problem for retailers in time. [4] investigate the inventory routing problem via the restless bandit framework. [35] study the admission control and routing of customers seeking service via assorted stations. [18] address the resource allocation among patients in a healthcare delivery system via restless multiarmed bandit models. [39] utilize a restless bandit formulation to dynamically allocate perishable inventories in a knapsack setting. [44] benefit from restless bandits to find the optimal screening strategy for hepatocellular carcinoma. [5] use restless bandits to study the

prioritization problem for hepatitis C treatment in United States prisons. Our work is aligned with the aforementioned papers in studying the allocation of limited resources among a large number of candidates in an individualized manner, and expands the scope of the literature by considering a regulatory compliance context.

Restless multi armed bandits have also been investigated in depth from a theoretical perspective over the past few decades. [68] defines the indexability property and provides a selection policy known as Whittle's index that prioritizes the arms at each time according to their states (states can be defined based on the arms' features). [67] show that Whittle's policy is asymptotically optimal except in rare instances and that the size of the suboptimality in these cases is negligible. [10] provide linear programming relaxations for restless bandit problems. [53] further investigates the indexability and optimality of restless bandits for problems satisfying partial conservation law. [32] study the two-armed restless bandits with imperfect information and derive their indexability. We prove the indexability of our RMAB formulation and derive its mathematical properties.

This work contributes to nascent research on environmental compliance monitoring in the operations management literature. [43] uses a game theory model to investigate the effect of the regulator's inspection policy (random and periodic) on one firm's noncompliance disclosure. [66] develops self-disclosure regulations for facilities' stochastic hazards. They aim to minimize the expected societal cost in the long run by dynamically determining the self-disclosure reward and inspection policy for the regulator. [2] model the interaction between a facility's self-policing strategy and the regulator's compliance restoration strategy, with a focus on the impact of Permanent Fix (PF) and Temporary Fix (TF) restoration policies on strategic interactions between the regulator and the firm. [46] empirically demonstrate the learning effect from inspections within and among facilities. Our contribution to this literature is to study environmental compliance monitoring strategies in a multiple-firm scenario under resource constraints. In addition to considering the resource constraints, we individualize the Compliance Monitoring Strategy by taking into account static and dynamic

firm characteristics. Furthermore, we validate the performance of our model using the EPA OECA compliance data set.

Our work has important implications for environmental regulators, and indicates the value of incorporating diverse attributes of the facility rather than only emission quantities in designing the optimal Compliance Monitoring Strategy and reducing harm to the environment and human health.

2.2 Model

We consider a regulator (e.g. EPA) who is responsible for ensuring that N facilities in a certain region are in compliance with environmental laws and regulations by means of inspections. We consider an infinite time horizon with discrete time periods. The compliance states of facilities evolve according to a (partially) *hidden* Markov chain. In each period, the regulator updates her belief that each facility is in compliance based on facility characteristics and past inspection history. Then, the regulator selects M facilities for inspection ($M < N$) and compels non-compliant facilities to get back into compliance. The objective of the regulator is to minimize the long-run average environmental cost caused by facilities that are not in compliance with regulations.

In the baseline model developed in this section, we assume that inspecting each facility requires the same amount of resources. We further assume that inspections are perfectly accurate, and fully capable of detecting existing violations.

2.2.1 Facilities' Compliance State Evolution

We start by defining the compliance states associated with a facility, which are unobservable to the regulator without inspection. A facility that abides by all the applicable environmental regulations, i.e. has no violations, is in *compliance* (denoted by C). Any deviation from the environmental regulations is considered in *non-compliance* or *violation*. Although any transgression from the applicable regulation is regarded as noncompliance and addressed

by the regulator, some violations can be more harmful to the environment and human health. In the Clean Air Act, the violations that (i) likely pose significant risk to public health or the environment through emitting air pollutants or (ii) hinder implementation of environmental regulations are called *High-priority Violations* (denoted by HPV) [23]. For instance, facilities that release hazardous air pollutants (e.g. methanol or toluene) are required to have appropriate control devices (e.g. thermal oxidizer or low temperature condenser) to reduce the hazards by 95% and turn pollutants to less damaging substances (water and carbon dioxide). Failing to utilize the appropriate control devices or improper working condition of these devices are examples of high priority violations. Falsifying environmental records is another example of HPV since it impedes the implementation of the environmental regulations. For ease of exposition, we label the rest of the violations which do not pose a major threat for the environment and public health as *Low-priority Violations* (denoted by LPV). Note that if instances of both low-priority and high-priority violations concurrently exist in a facility, the state is considered HPV.

Upon the detection of any type of violation, the regulator requires the facility to restore full compliance. As such, the non-compliant facility should design a plan for fixing the violations in a timely manner with the regulator's agreement. The time between the detection of noncompliance and restoration of full compliance is called *Restoration* (R). We define the restoration state (R) only as the formal restoration process taking place after the violation is explicitly observed by the regulator. Therefore, although facilities might fix the violation on their own without inspection, we do not consider this to be the restoration state. Since the restoration from the high-priority violations may require more time and effort than low-priority ones, we define two restoration states: *Restoration from LPV* (R^{LPV}) and *Restoration from HPV* (R^{HPV}).

In sum, a facility can be in one of the following five states with respect to environmental regulations at any given time: compliance (C), low priority violation (LPV), high priority violation (HPV), restoration from LPV (R^{LPV}) or restoration from HPV (R^{HPV}).

We assume that the facilities' states alternate according to a discrete-time Markov chain. The transition probabilities between the states for facility $n = 1, 2, \cdots, N$ are exogenous and known to the regulator. States C, LPV and HPV are unobservable (hidden) unless through inspection, while the restoration states are visible because they follow the detection of non-compliance and the facility is monitored by the regulator until it achieves compliance again. In Section 2.5, we estimate these transition probabilities based on facility attributes such as location, size, type of industry, type of hazardous emissions, etc.

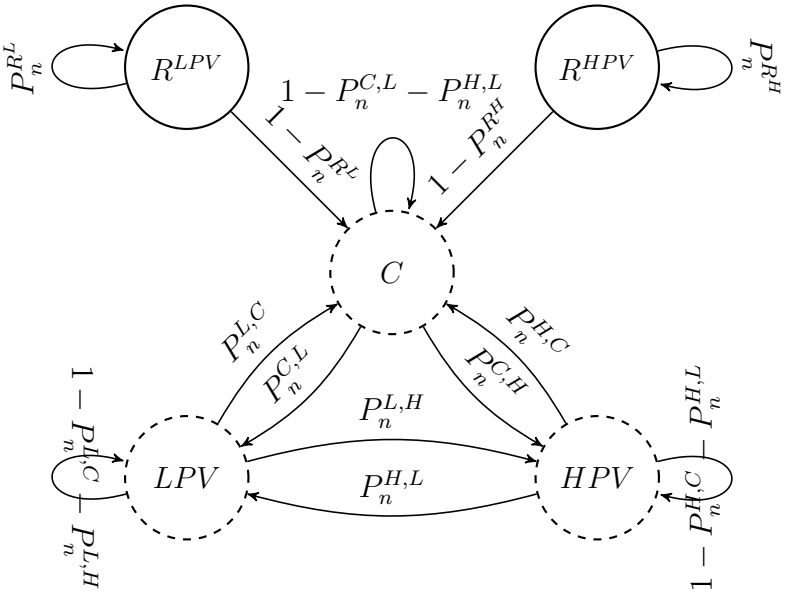

Figure 2.1: Hidden Markov chain transition probabilities of facility n when it is not inspected (NI) in a period.

Figure 2.1 depicts the Markov chain transition probabilities for facility n in a period when it is not inspected. If the facility had been previously inspected and found to be non-compliant, it may be in one of the restoration states, and stays there until it achieves compliance. Otherwise, it transitions on its own between compliance, low priority, and high priority violation states until the next inspection. Here, return to compliance without inspection captures internal self-policing and compliance efforts by firms [43, 2].

Otherwise, suppose facility n is inspected (I) in a certain period. If the facility is found

to be non-compliant, i.e., in states LPV or HPV, the state transitions to the corresponding restoration state R^{LPV} or R^{HPV} in the next period. If it is found to be compliant in the current period, it may stay compliant or may transition to a low- or high-priority violation in the next period. The state transition probabilities are shown in Figure 2.2.

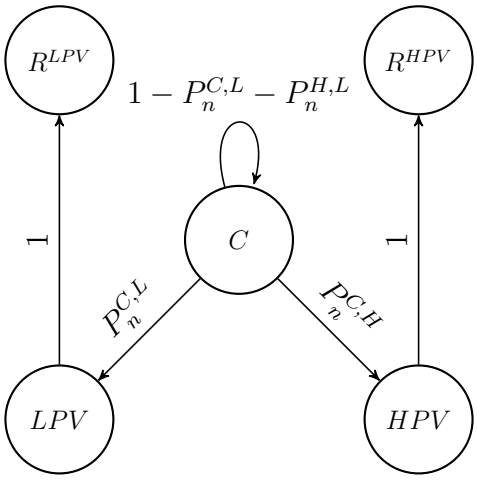

Figure 2.2: Hidden Markov chain transition probabilities of facility n if it is inspected (I) in a period.

If facility n is noncompliant (LPV or HPV), it creates an expected environmental cost of $\mathbf{c}_n = (c_n^L, c_n^H)$ per period. We assume that the environmental cost during the restoration stage is lower, and normalize it to zero without loss of generality.

2.2.2 Regulator's Observable Markov Chain and the Restless Multiarmed Bandit Formulation

Next, we consider the state of facilities $n = 1, 2, \cdots, N$ from the regulator's perspective. For any facility n, if it has been found in violation and is currently in the restoration process (R^{LPV} or R^{HPV}), we assume its state is observable to the regulator: In practice, regulators such as EPA will closely monitor facilities found to be non-compliant until they reach compliance. If facility n is not in the restoration process, let s_n be the number of periods since the facility's last known time of compliance. This corresponds to either the last time

that the facility was inspected and found to be compliant, or the last time the facility became compliant following a restoration process. We assume that, due to environmental regulations, s_n is restricted to be less than T periods. Namely, any facility must be inspected at most T periods after its last inspection or its last restoration to compliance, whichever is more recent. Therefore, from the regulator's perspective, his observable state space consists of $s_n \in \{1, 2, \cdots, T\} \cup \{R^{LPV}, R^{HPV}\}$ for facility n. At the beginning of the time horizon, we assume all facilities are in compliance.

If facility n is not inspected, the observable state transition probabilities for this facility are shown in Figure 2.3. If the state is $s \in \{1, \cdots, T-1\}$, it increases to $s+1$. If the state is R^{LPV} or R^{HPV}, there is either a self-transition into the same state, or the facility becomes compliant so that the next state is $s = 1$. Note that we do not specify a transition out of state T, because an inspection is required in this state.

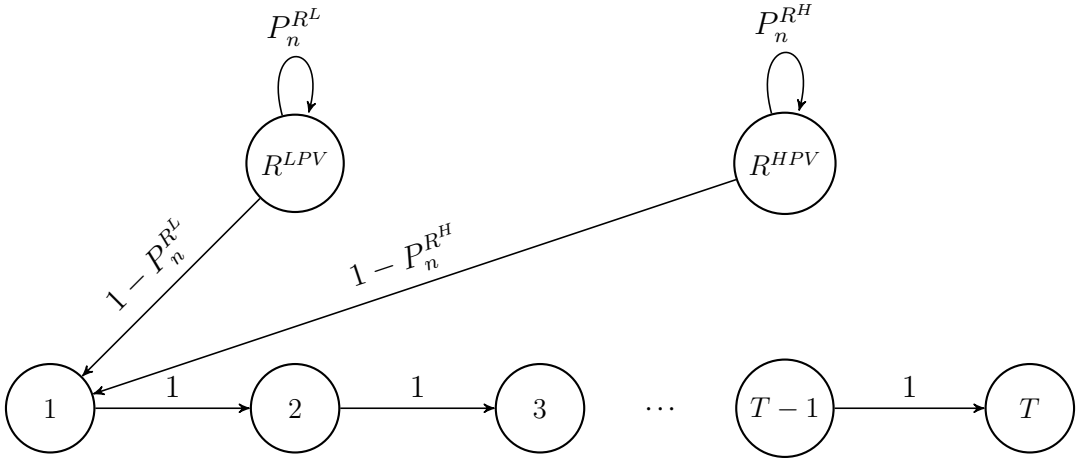

Figure 2.3: Observable Markov chain transition probabilities of facility n in a period with no inspection (NI).

If facility n is inspected, the observable state transition diagram and the associated transition probability matrix for this facility are shown in Figures 2.4 and 2.5, respectively. If the state is $s \in \{1, \cdots, T\}$, an inspection will either discover compliance or a violation. Let the probability of facility n being in state C, LPV or HPV be denoted by the vector

$\mathbf{q}_n(s) = (q_n^C(s)), q_n^L(s), q_n^H(s))$. These three probabilities are the transition probabilities from s into 1, R^{LPV} and R^{HPV}, respectively. Here, $\mathbf{q}_n(s)$ is computed as $(1,0,0)^\top (Q_n)^s$, where Q_n is the state transition probability matrix corresponding to the class of states C, LPV and HPV in the hidden Markov chain depicted in Figure 2.1. Note that we define the outgoing transition probabilities from states R^{LPV} and R^{HPV} to be the same as those under the no inspection case; thus, it is never optimal to inspect a facility during a restoration period. We make the following assumption on the probability of violations.

Assumption 1 *For any facility $n \in \{1, \cdots, N\}$, the probabilities of low and high priority violations ($q_n^L(s)$ and $q_n^H(s)$) are increasing in $1 \leq s \leq T$.*

This is a mild assumption, since the probability of violation is likely to increase over time if the regulator does not inspect a facility.

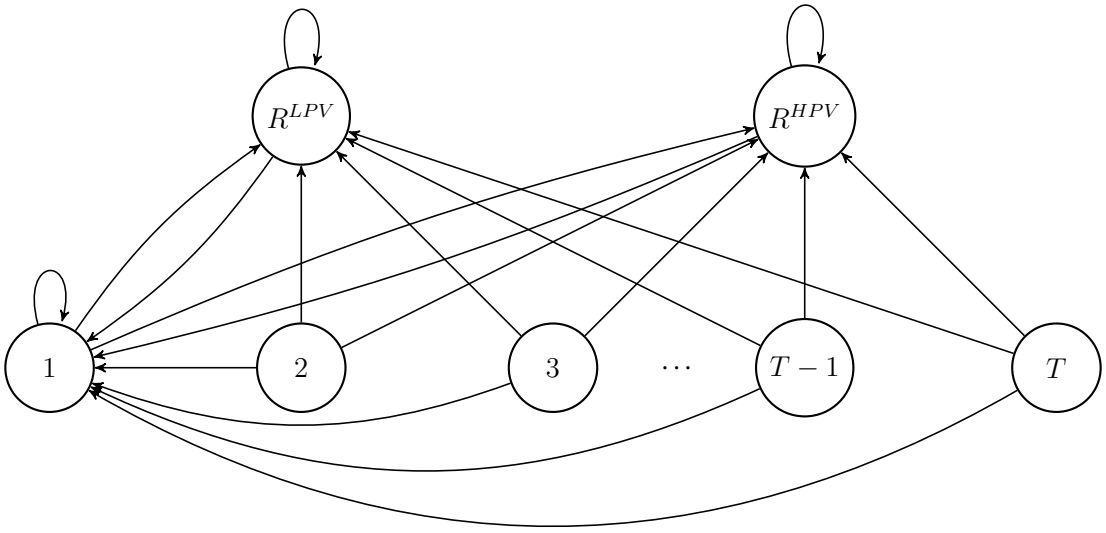

Figure 2.4: Observable Markov chain transition probabilities of facility n in a period with inspection (I).

Given the observable Markov chains for the N facilities, we formulate the decision problem faced by the regulator as a restless multiarmed bandit (RMAB) model [68]. The restless bandit setting includes N arms, which correspond to N facilities in our setting. In

$$
\begin{array}{c}
 \\
1 \\
2 \\
3 \\
... \\
T-1 \\
T \\
R^{LPV} \\
R^{HPV}
\end{array}
\begin{array}{c}
\begin{array}{ccccccccc}
1 & 2 & 3 & ... & T-1 & T & R^{LPV} & R^{HPV}
\end{array} \\
\left(\begin{array}{ccccccccc}
q_n^C(1) & 0 & 0 & ... & 0 & 0 & q_n^L(1) & q_n^H(1) \\
q_n^C(2) & 0 & 0 & ... & 0 & 0 & q_n^L(2) & q_n^H(2) \\
q_n^C(3) & 0 & 0 & ... & 0 & 0 & q_n^L(3) & q_n^H(3) \\
... & ... & ... & ... & ... & ... & ... & ... \\
q_n^C(T-1) & 0 & 0 & ... & 0 & 0 & q_n^L(T-1) & q_n^H(T-1) \\
q_n^C(T) & 0 & 0 & ... & 0 & 0 & q_n^L(T) & q_n^H(T) \\
1-P_n^{R^L} & 0 & 0 & ... & 0 & 0 & P_n^{R^L} & 0 \\
1-P_n^{R^H} & 0 & 0 & ... & 0 & 0 & 0 & P_n^{R^H}
\end{array}\right)
\end{array}
$$

Figure 2.5: Observable Markov chain transition probabilities of facility n in a period with inspection (I).

each period, M arms are selected by the decision maker to be active (i.e. inspected), and the rest $N - M$ arms stay passive (i.e. not inspected). In other words, the decisions in each period must satisfy $\{a_n \in \{I, NI\} : \sum_{n=1}^{N} \delta(a_n = I) = M\}$.

An environmental cost is incurred in each period. Recall that c_n^L and c_n^H are the per period cost at facility n in states LPV and HPV, and that the cost for the restoration states is normalized to 0. Therefore, regardless of whether arm n is activated, the one-period expected environmental cost associated with state s_n is given by $\mathbf{c}_n^\top \cdot \mathbf{q}_n(s_n) = (0, c_n^L, c_n^H)^\top \cdot (q_n^C(s), q_n^L(s), q_n^H(s))$. The decision maker's objective is to minimize the long-run average cost over an infinite horizon.

2.3 An Index-Based Inspection Policy

The restless bandit problem is well known to be computationally challenging, as the problem state space grows exponentially with the number of arms. [56] showed that the restless bandit problem is PSPACE-hard even if all bandits follow a deterministic transition. To make computation for the restless bandit problem tractable, index policies have been introduced. Whittle's index is one of the most widely used among this class of policies [68]. To be able to use this index policy, we need to prove that the *indexability* condition holds. However,

verifying the indexability condition is challenging in general [37]. If the indexability condition holds and the ratio M/N remains fixed, it is shown by [67] that under some technical conditions, Whittle's index policy is asymptotically optimal as the number of arms N goes to infinity (without this technical condition, counterexamples exist but are rare). In this section, we start by reviewing the definitions of Whittle's index policy and the indexability condition. We then prove indexability for our facility inspection problem and analyze the structure of the resulting heuristic.

2.3.1 Definitions of Indexability and Whittle's Index

The heuristic policy by [68] considers a relaxation procedure as follows: Let $M(t)$ be the number of arms which are active at period t. The original problem requires that exactly M arms are activated, i.e., $M(t) = M$. Whittle's approximation only requires this condition to hold in expectation: $E[M(t)] = M$. Then a Lagrangian relaxation is applied to this expectation constraint. Let v be its Lagrangian multiplier. With the relaxation, the regulator is allowed to inspect an unlimited number of facilities in a period, although it must pay an "activation fee" or a "virtual inspection cost" that is equal to v for each inspected facility.

Using Lagrangian relaxation, the inspection decision problem is now *separable* for each facility. Specifically, given v, the optimal inspection problem for any facility n is a dynamic program with two actions: inspect (I) or not inspect (NI); if the decision is I, an extra cost of v is incurred. We are now ready to define the indexability condition.

Definition 1 (Indexability) *Let $\mathcal{S}_n(v)$ be the set of states for which it is optimal not to inspect facility n given activation cost v. We call the problem* indexable *if $\mathcal{S}_n(v) \subset \mathcal{S}_n(v')$ for any $v < v'$ and any facility n.*

Definition 2 (Whittle's Index) *For each facility n,* Whittle's index *for state s is $v_n(s) = \inf\{v : s \in \mathcal{S}_n(v)\}$.*

Definition 1 states that a facility is indexable if the set of states for which no inspection

is optimal increases monotonically as the activation fee increases. Definition 2 means that Whittle's index associated with each state is the break-even point where the decision maker is indifferent between inspection and no inspection.

Remark 1 *Throughout this chapter, the term "increasing" (resp., "decreasing") is defined in the general sense and is interchangeable with the word "nondecreasing" (resp., "nonincreasing").*

2.3.2 Proof of the Indexability Condition

Next, we prove the indexability condition and show how to compute the indices of facilities. We focus on a given facility $n \in \{1, \cdots, N\}$.

As a first step, we formulate the dynamic program given the value of Lagrangian multiplier (i.e., inspection cost) v. Recall that $\mathbf{q}_n(s) = (q_n^C(s), q_n^L(s), q_n^H(s))$ denote the probabilities of facility n being in states C, LPV, and HPV for $s \in \{1, \cdots, T\}$ and that $\mathbf{c}_n = (0, c_n^L, c_n^H)$ denote the associated expected environmental costs. Using the transition diagrams from Figures 2.3 and 2.4, we obtain the Bellman's equations for the average cost dynamic program as

$$\gamma_n + h_n(s) \;=\; \mathbf{c}_n^\top \mathbf{q}_n(s) + \min\big\{\mathbf{g}_n^\top \mathbf{q}_n(s) + v,\; h_n(s+1)\big\}, \qquad \forall s \in \{1, \cdots, T-1\}, \tag{2.1a}$$

$$\gamma_n + h_n(T) \;=\; \mathbf{c}_n^\top \mathbf{q}_n(T) + \mathbf{g}_n^\top \mathbf{q}_n(T) + v, \tag{2.1b}$$

$$\gamma_n + h_n(R^{LPV}) \;=\; (1 - P_n^{R^L}) h_n(1) + P_n^{R^L} h_n(R^{LPV}), \tag{2.1c}$$

$$\gamma_n + h_n(R^{HPV}) \;=\; (1 - P_n^{R^H}) h_n(1) + P_n^{R^H} h_n(R^{HPV}). \tag{2.1d}$$

Here, γ_n is the optimal long run average cost associated with facility n given inspection cost v. We use $h_n(s)$ to denote the differential cost of state $s \in \{1, \cdots, T\} \cup \{R^{LPV}, R^{HPV}\}$. We also denote by $\mathbf{g}_n = (h_n(1), h_n(R^{LPV}), h_n(R^{HPV}))$ the vector of differential costs starting from state $s = 1, R^{LPV}, R^{HPV}$, respectively. Eq (2.1a) is the Bellman's equation

associated with state $s = \{1, \cdots, T-1\}$: If the decision is "inspection," an inspection cost v is incurred, and the next state can be either 1, R^{LPV} or R^{HPV} (if the facility is found to be in states C, LPV or HPV upon inspection, respectively), with probability vector $\mathbf{q}_n(s)$; if the decision is "no inspection," the next state is simply $s+1$. In Eq (2.1b), when a facility is in state T, it must be inspected according to our assumption. In Eqs (2.1c) and (2.1d), the facility is in restoration from violations LPV or HPV and will return to compliance with the associated probability.

Remark 2 *The Bellman's equation for infinite horizon average cost problem requires certain assumptions. One such assumption is that there exists a special state such that for all initial states and all policies, this special state will be visited infinitely often [9]. This assumption holds in our setting, as the state $s = 1$ (one period after last known compliance) will be visited infinitely often under any policy and any starting state.*

There is an extra degree of freedom in the Bellman's equations (2.1a)-(2.1d), so we normalize the differential costs by letting $h_n(1) = 0$. The equations (2.1c) and (2.1c) for recovery states can be simplified as

$$h_n(R^{LPV}) = -\frac{\gamma_n}{1 - P_n^{R^L}}, \quad h_n(R^{HPV}) = -\frac{\gamma_n}{1 - P_n^{R^H}}. \tag{2.2}$$

In what follows, we prove that the indexability condition holds in our problem by using the following lemma. We write the differential cost $h_n(s)$ as $h_n(s, v)$ to emphasize that it depends on the virtual inspection cost v.

Lemma 1 *The function $\tilde{h}_n(s, v) := h_n(s, v) - \mathbf{g}_n^\top \mathbf{q}_n(s-1) - v$ is decreasing in v for any $s = 1, \cdots, T$.*

Using Lemma 1 and Equation (2.1a), we immediately have the following result.

Theorem 1 *For a given facility n, the set of states for which "no inspection" is optimal satisfies $\mathcal{S}_n(v) \subset \mathcal{S}_n(v')$ for any $v < v'$, implying that the restless bandit model is indexable.*

2.3.3 Whittle's Index Policy for Multiple Facilities

If the indexability condition holds, we can apply a simple heuristic policy: in each period, rank the N facilities according to their Whittle's indices given current states and choose the top M facilities to be inspected.

Upon proving the indexability of our problem, we can conclude that Whittle's index policy is asymptotically optimal as the number of facilities N and the inspection capacity M both go to infinity, while their ratio M/N remains a constant [67].

Simulating Whittle's index policy for multiple facilities with heterogeneous compliance transition rates, we observe that the optimal inspection strategy for multiple facilities is not cyclic (Figure 2.6). This is opposed to the EPA Compliance Monitoring Strategy that suggests periodic inspections.

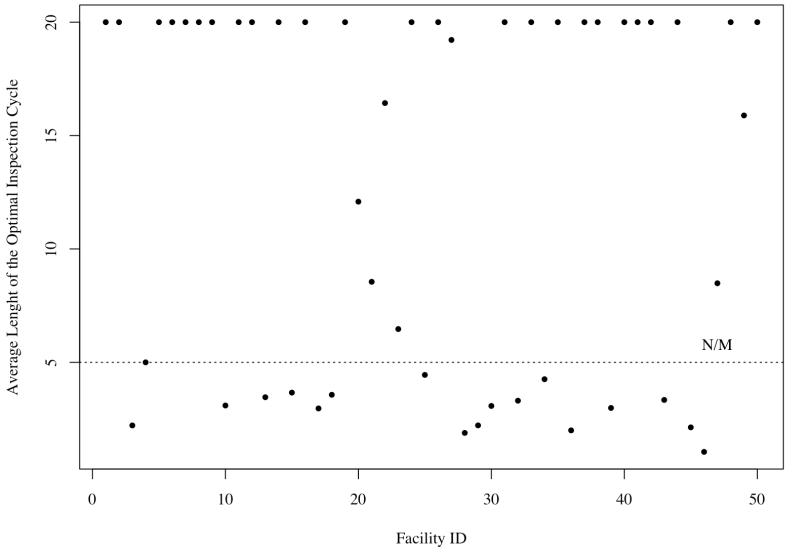

(a) Mean (benchmark: uniform cyclic policy ($N/M = 5$)).

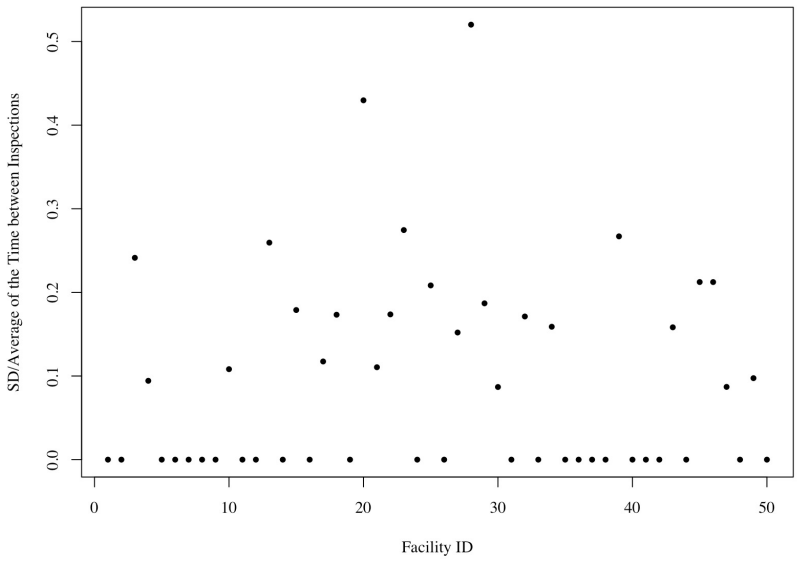

(b) Standard deviation over the mean

Figure 2.6: Plots of the mean and standard deviation over the mean of the time intervals between two consecutive Whittle's index suggested inspections for each facility ($N = 50$, $M = 10$, and $T = 20$).

2.4 Extensions

In this section, we consider two extensions to the main model: heterogeneous inspection costs and the possibility of a major environmental adverse event ("disaster").

2.4.1 Inspections with Heterogeneous Resource Requirements

In the main body of the chapter, we assumed there is a constraint on the number of facilities that can be inspected in each period. More generally, inspecting different facilities may require different levels of resources depending on facility characteristics (e.g., location, type of industry, size, etc), and facilities to inspect could be determined based on a total budget. Let w_n be the level of resource required to inspect the n^{th} facility, and that there is a total resource constraint R in each period. Then the index policy can be modified to select facilities with the largest indices within the available resource constraint.

$$\text{Max} \quad \Sigma_{i=1}^{N} \gamma_n(t) x_n$$

$$\Sigma_{i=1}^{N} w_n x_n \leq R$$

$$x_n \in \{0, 1\}$$

where $\gamma_n(t)$ denotes the index of the facility n at time t.

2.4.2 Disaster Occurrence

Failing to address high priority violations might result in a *disaster* (D) which is immediately observable by the regulator and citizens even without conducting an inspection. For example, Tonawanda Coke Corporation (TCC) located in Tonawanda, NY, was reported by local citizens to the EPA after they observed dark smokey discharge in its surroundings. The facility was found to be over-emitting cancer causing substances including benzene [70]. Restoration from the *disaster* state demands significantly more effort compared to restoration from LPV or HPV. Therefore, we differentiate between these states, and define R^D as restoration from the *disaster* state. *Disaster* (D) and its associated recovery (R^D) along with the R^{LPV} and R^{HPV} are observable by the regulator. C, LPV and HPV are the hidden states as described in the main model. The hidden Markov chain transition probabilities of facility n without and with inspection are depicted in Figures 2.7 and 2.8. As shown here, upon the detection of any type of violation (through inspection or occurrence of disaster), the facility switches to the corresponding restoration state until it is back to compliance.

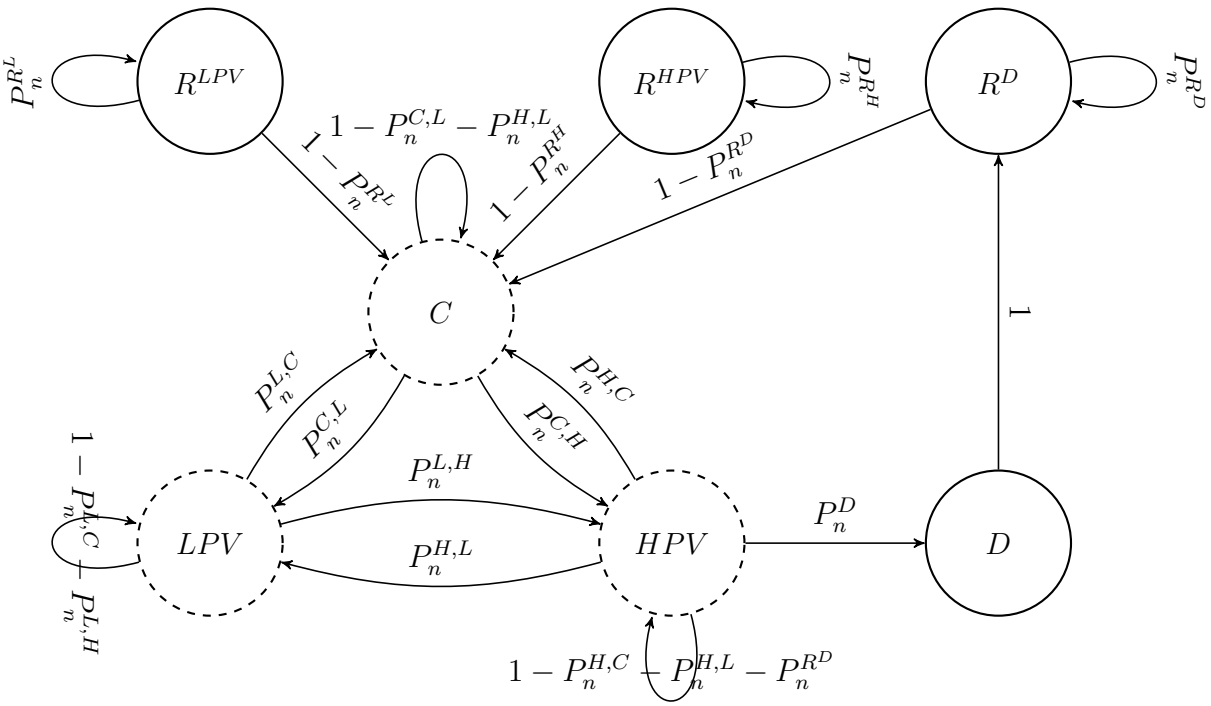

Figure 2.7: Hidden Markov chain transition probabilities of facility n if it is not inspected (NI) in a period (Disaster Included).

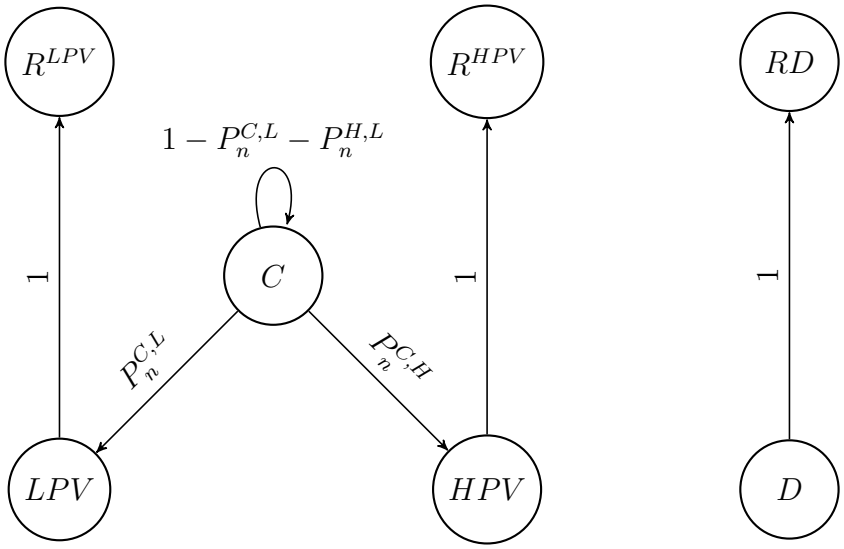

Figure 2.8: Hidden Markov chain transition probabilities of facility n if it is inspected (I) in a period (Disaster Included).

From the perspective of the regulator, the observable Markov chain transition probabilities are shown in Figures 2.9 and 2.10, respectively. As shown, the regulator's observable state space includes $s_n \in \{1, 2, \cdots, T\} \cup \{D, R^{LPV}, R^{HPV}, R^D\}$ for facility n.

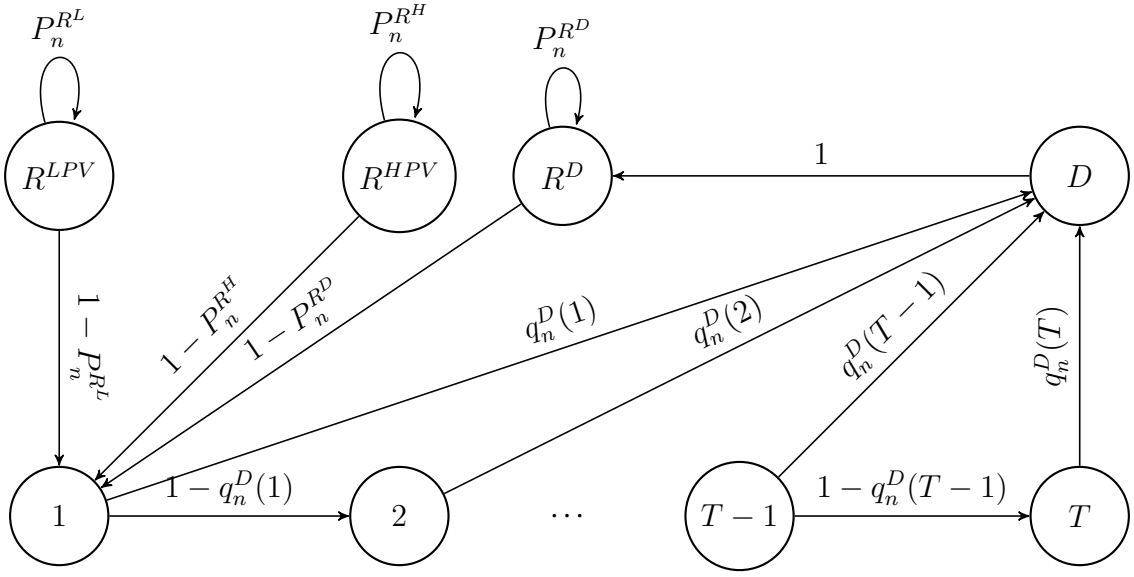

Figure 2.9: Observable Markov chain transition probabilities of facility n in a period with no inspection (NI) (Disaster Included).

The Bellman's equation corresponding to the described model can be written as Eq. 2.3.

$$\gamma_n + h_n(s) = \mathbf{c}_n^\top \mathbf{q}_n(s) + \min\big\{\mathbf{g}_n^\top \mathbf{q}_n(s) + q_n^D(s)h_n(D) + v,\ (1 - q_n^D(s))h_n(s+1) + q_n^D(s)h_n(D)\big\} \qquad s \in \{1, \cdots, T-1\}, \tag{2.3a}$$

$$\gamma_n + h_n(T) = \mathbf{c}_n^\top \mathbf{q}_n(T) + \mathbf{g}_n^\top \mathbf{q}_n(T) + q_n^D(T)h_n(D) + v, \tag{2.3b}$$

$$\gamma_n + h_n(D) = c_n^D + h_n(R^D), \tag{2.3c}$$

$$\gamma_n + h_n(R^{LPV}) = (1 - P_n^{R^L})h_n(1) + P_n^{R^L}h_n(R^{LPV}), \tag{2.3d}$$

$$\gamma_n + h_n(R^{HPV}) = (1 - P_n^{R^H})h_n(1) + P_n^{R^H}h_n(R^{HPV}), \tag{2.3e}$$

$$\gamma_n + h_n(R^D) = (1 - P_n^{R^D})h_n(1) + P_n^{R^D}h_n(R^D). \tag{2.3f}$$

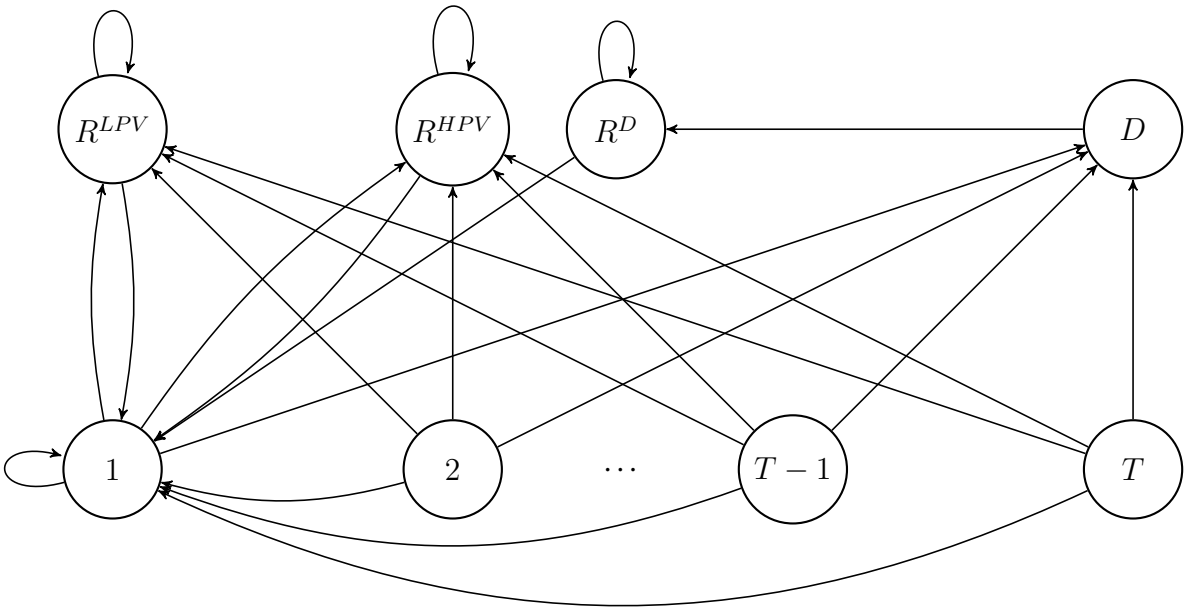

Figure 2.10: Observable Markov chain transition probabilities of facility n in a period with inspection (I) (Disaster Included).

$$
\begin{array}{c}
 \\
1 \\
2 \\
3 \\
... \\
T-1 \\
T \\
D \\
R^{LPV} \\
R^{HPV} \\
R^D
\end{array}
\begin{array}{c}
\begin{array}{cccccccccc}
1 & 2 & 3 & ... & T-1 & T & D & R^{LPV} & R^{HPV} & R^D
\end{array} \\
\left(\begin{array}{cccccccccc}
q_n^C(1) & 0 & 0 & ... & 0 & 0 & q_n^D(1) & q_n^L(1) & q_n^H(1) & 0 \\
q_n^C(2) & 0 & 0 & ... & 0 & 0 & q_n^D(2) & q_n^L(2) & q_n^H(2) & 0 \\
q_n^C(3) & 0 & 0 & ... & 0 & 0 & q_n^D(3) & q_n^L(3) & q_n^H(3) & 0 \\
... & ... & ... & ... & ... & ... & ... & ... & & \\
q_n^C(T-1) & 0 & 0 & ... & 0 & 0 & q_n^D(T-1) & q_n^L(T-1) & q_n^H(T-1) & 0 \\
q_n^C(T) & 0 & 0 & ... & 0 & 0 & q_n^D(T) & q_n^L(T) & q_n^H(T) & 0 \\
0 & 0 & 0 & ... & 0 & 0 & 0 & 0 & 0 & 1 \\
1-P_n^{R^L} & 0 & 0 & ... & 0 & 0 & 0 & P_n^{R^L} & 0 & 0 \\
1-P_n^{R^H} & 0 & 0 & ... & 0 & 0 & 0 & 0 & P_n^{R^H} & 0 \\
1-P_n^{R^D} & 0 & 0 & ... & 0 & 0 & 0 & 0 & 0 & P_n^{R^D}
\end{array}\right)
\end{array}
$$

Figure 2.11: Observable Markov chain transition probabilities of facility n in a period with inspection (I) (Disaster Included).

Consistent with Eq 2.1, γ_n is the long run average optimal cost associated with facility n given inspection cost v, and $h_n(s)$ is the differential cost starting from state s, with

$h_n(1) = 0$. Further, the facility should get inspected at most T periods after the last known compliant state (Eq. 2.3b). When a facility transitions to a disaster state, this is detectable without inspection and imposes a large cost c_n^D on the environment $c_n^D \gg c_n^L, c_n^H$ (Eq. 2.3d). Equations 2.3d-2.3f capture the transitions associated with restoration from states LPV, HPV and D. Bellman's equation 2.3 for these states can be rewritten as Eq. 2.4:

$$h_n(R^L) = -\frac{\gamma_n}{1 - P_n^{R^L}}, \quad h_n(R^H) = -\frac{\gamma_n}{1 - P_n^{R^H}}, \quad h_n(R^D) = -\frac{\gamma_n}{1 - P_n^{R^D}}. \tag{2.4}$$

We now proceed to prove the indexability of the model. This proof requires a slightly more restricted version of Assumption 1 presented as Assumption 2.

Assumption 2 *The violation probabilities $q_n^L(t)$, $q_n^H(t)$ and $q_n^D(t)$ at any given time t are such that*

- *For LPV noncompliance, $q_n^L(t) \geq \frac{q_n^L(t-1)}{1-q_n^D(t-1)}$ or equivalently $(1 - q_n^D(t-1))q_n^L(t) - q_n^L(t-1) \geq 0$.*
- *For HPV noncompliance, $q_n^H(t) \geq \frac{q_n^H(t-1)}{1-q_n^D(t-1)}$ or equivalently $(1 - q_n^D(t-1))q_n^H(t) - q_n^H(t-1) \geq 0$.*

Assumption 2 tightens Assumption 1 as it imposes a non-negative lower bound on the increase in probabilities of low priority and high priority violations.

Lemma 2 *Under the Assumption 2, the function $\tilde{h}_n(s, v) := (1 - q_n^D(s-1))h_n(s, v) - \mathbf{g}_n^\top \mathbf{q}_n(s-1) - v$ is decreasing in v for any $s = 1, 2, ..., T$.*

Based on the Lemma 2 and Eq. 2.3, we have the following theorem that demonstrates indexability.

Theorem 2 *For a given facility n, the set of states for which "no inspection" is optimal satisfies $\mathcal{S}_n(v) \subset \mathcal{S}_n(v')$ for any $v < v'$, implying that the restless bandit model is indexable.*

2.5 Model Calibration

In this section, we calibrate the compliance monitoring model presented in §2.2 using the data from EPA's Clean Air Act (CAA) Monitoring program. The data can be accessed publicly at EPA's ICIS-Air database. We provide an overview of this dataset in §2.5.1 and describe the EPA current practice in §2.5.2. We then use the data to calibrate the MDP model in §2.5.3. The model calibration results will be used in the §2.6 to test different compliance monitoring policies.

2.5.1 Data Description

We use data for on-site inspections conducted through the Clean Air Act (CAA) program of the Environmental Protection Agency (EPA). The data set contains facilities' information and their compliance, and enforcement history during 2002-2016.[1] Because of the large scale of the data, we restrict our analysis to one of the ten EPA regions: Region 2, which covers New York, New Jersey, the U.S. Virgin Islands, and Puerto Rico.

There are a total of 19,374 facilities in Region 2 that are registered in the EPA's database. We exclude facilities with unknown, not applicable, and other emission size (476 facilities in total) from this statistics. Since EPA has not kept track of the facilities operating status, we assume that all the facilities currently registered in EPA data set were operating during the time frame from 2002-2016. All the facilities are classified by EPA into three main categories by size: major, synthetic minor (SMI) and minor.

We limit our analysis to the major and SMI facilities, mainly because the data for minor facilities are limited as they are inspected less frequently — only 34.09% of the minor facilities have been inspected at least once in the data set. Furthermore, minor facilities are potentially less harmful to the environment and public health due to the small size.

By excluding the minor facilities, the remaining data set consists of 5,156 facilities, in

[1] We do not include more recent data as the inspection history and enforcement actions data set after 2016 may be incomplete and still being updated.

which 833 are major and 4,323 are SMI (see a summary in Table 2.2).

To develop a comprehensive individualized compliance monitoring strategy, we extract the following information from the data set:

- **Facilities' characteristics**: Facility ID, type of industry, type of ownership, facilities' emission programs information, location, and demographics. For location, we use both county name and the non-attainment are flag. We use county as the measure for facility location over zip code, city, and state. County is detailed enough to provide insight about the location (unlike state) and aggregated enough to avoid excessive levels in our estimation procedure (unlike city or zip code). Non-attainment area flag is another information about the location which determines if the area has air quality worse than the national ambient air quality standards [28]. To represent demographics, we use the environmental justice area flag. Environmental justice areas refer to the census blocks where at least 20% of residents are in poverty, or at least 30% of them are minority [3]. All of the fields are categorical, Table 2.1 provides a summary of these features.

- **Inspection history:** The history of the on-site inspections/off-site monitorings performed on the facilities, whether they have been conducted by EPA or states, the type of inspection/monitoring (on-site/off-site and full/partial inspection), and air programs included in the inspection/monitoring. Note that we only focus on on-site inspections, we also do not differentiate between full and partial inspections, and inspections conducted through EPA and states.

- **Violation enforcement history:** The history of the enforcement actions given to each facility, including the date that settlement has been entered, the amount of penalty, and whether the enforcement activity was judicial or administrative. We do not differentiate between judicial and administrative enforcement actions.

For more explanation of the fields in data set see `https://echo.`

epa.gov/tools/data-downloads/icis-air-download-summary#air-program-codes), the detailed data processing steps are also provided in Appendix §B.

Table 2.1: Facilities' characteristics and their number of levels.

Facility feature	Major	SMI
Type of industry	46	78
Facility ownership type	8	8
Applicable air programs	21	19
County name	108	99
Non-attainment area flag	2	2
Environmental justice area flag	2	2

Identifying Regular vs. Restoration Inspections.

We categorize all the conducted inspections to two groups of *regular* and *restoration* inspections. Regular inspections are the planned inspections performed on the facilities when the last known state of the facility is compliant. Upon detecting noncompliance (NC: LPV or HPV) through inspection, the facility is required to design an effective compliance restoration plan under the supervision of the regulator, following which the regulator may conduct a restoration inspection as follow up to assure the compliance achievement.[2]. Therefore, restoration inspections are performed when the last known state of the facility is noncompliant.

Table 2.2, provides an overview of the regular inspections conducted on the major and SMI facilities of the EPA Region 2 during 2002-2016.

Remark 3 *Note that throughout this chapter, we only allocate resources (select facilities) for regular inspections since restoration inspections may be conducted based on the regulator discretion following observed violations anyways.*

[2]Note that in practice these inspections may be conducted as multiple partial inspections through the violation restoration interval. For low priority violations, restoration inspections happen within 6 months following the noncompliant inspection. This period may be longer for HPVs. More information on restoration inspections and how we use them is provided in §B.2.2.

Table 2.2: Conducted Regular Inspections Statistics for EPA Region 2 during 2002-2016.

		Major	SMI
Facilities	Number of facilities	833	4323
Inspections	Total number of regular inspections	6370	7467
	Number of facilities with at least one regular inspection	811	3275
	Average number of regular inspections per facility	7.65	1.73
	Average time between two regular inspections (weeks)	85.04	181.16
Violations	Percentage of LPVs in regular inspections	9.65%	3.94%
	Percentage of HPVs in regular inspections	1.62%	0.98%
	Percentage of all violations in regular inspections	11.27%	4.92%

2.5.2 Characterizing the Current Practice

The United States federal Compliance Monitoring Strategy recommends periodic inspections with recommended, at a minimum, two-year and five-year intervals for majors and SMI facilities, respectively [24]. We use this policy as one of the benchmarks in the §2.6. As presented in Table 2.2, the average time between regular inspections for major and SMI facilities are respectively 85.04 and 181.16 weeks, which are shorter than the recommended intervals.

2.5.3 Characterizing the Compliance and Restoration Transition Probabilities

We divide the parameters that we require to estimate into two categories of restoration and compliance transition probabilities. To increase our estimation's reliability, we cluster the facilities of each emission size (major and SMI) and perform the parameter estimation in the aggregated (cluster) level. We estimate these parameters in a two-fold process as follows:

- We initially use the hierarchical clustering analysis (HCA) to divide the facilities into k clusters based on their characteristics (Table 2.1). The goal of clustering is to find groups of facilities more similar to each other. The following steps are required to this end:

  - Choosing the dissimilarity (distance) matrix: Selecting an appropriate dissimilarity

measure is a fundamental step in clustering. We use the features of Table 2.1 as input for the dissimilarity analysis. Facilities' characteristics are categorical, we select Gower's distance measure to determine the distance between facilities' characteristics [38].

- Choosing the clustering algorithm: Hierarchical clustering is commonly implemented as agglomerative (bottom-up), which starts with treating each observation as a distinct cluster, and proceeds by merging the most similar clusters in each step according to their intergroup dissimilarity measure. We use the agglomerative hierarchical clustering with Ward's minimum variance linkage which resulted in the most balanced clusters among common hierarchical clustering techniques (complete, average, and minimax linkage agglomerative HCA). The Ward's minimum variance linkage agglomerative hierarchical clustering minimizes the total within-cluster variance. This approach initiates with considering each point as a single cluster. Each further step merges the pair of clusters that cause the minimum increase in total within-cluster variance upon aggregation. For more information, see [52].

- Choosing the number of clusters and assessing them: We use the Elbow method (traced to [63]) for selecting the optimal number of clusters for Ward's minimum variance linkage agglomerative clustering of major and SMI facilities.

- We subsequently estimate parameters (restoration and compliance transition probabilities) for each cluster. We aggregate observations for each cluster and estimate a single set of parameters. In other words, facilities within a cluster all have the same set of parameters.

We discuss the approach for determining number of clusters next.

Determining the Number of Clusters.

Figures 2.12 depict the plots of the within clusters sum of squares versus number of clusters (1 to 15 clusters) for the Ward's minimum variance linkage agglomerative hierarchical clustering of major and SMI facilities. In both plots, we observe an elbow after which increasing the number of clusters (further splitting) would only bring minor decrease in the within-clusters sum of squares. The location of the elbows suggest five clusters for major facilities (Figure 2.12a) and around seven clusters for SMI facilities (Figure 2.12b). Therefore, we select five and seven as the optimal number of clusters for Ward's minimum variance linkage agglomerative hierarchical clustering of major and SMI facilities, respectively.

Estimation of the Restoration Transition Probabilities.

We then estimate restoration from low priority (P^{R^L}) and high priority violations (P^{R^H}). Appendix §B.2.2 provides detail of estimation of restoration parameter estimations. Table 2.3 presents overview of average restoration time for major and synthetic minor facilities of Region 2 facilities.

- Major Facilities: Major facilities require, on average, 11.04 and 95.31 weeks to restore from low priority and high priority violations, respectively.
- Synthetic Minor (SMI) Facilities: It takes, on average, 10.32 and 65.74 weeks for SMI facilities to restore compliance from LPV and HPV violations, respectively.

Table 2.3: Average restoration time statistics for EPA Region 2 facilities during 2002-2016.

Average restoration time (weeks)	Major	SMI
Low priority violations	11.04	10.32
High priority violations	95.31	65.74

Restoration time from low (high) priority violations can be modeled with a geometric distribution. Thus, for each facility cluster, we have:

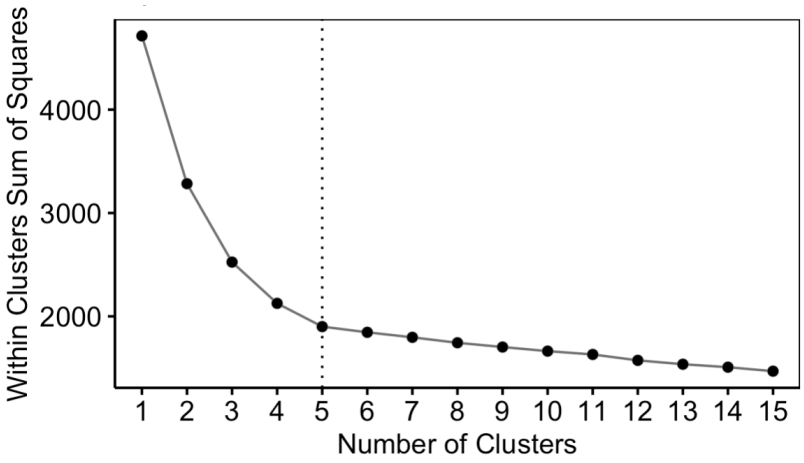

(a) Major facilities

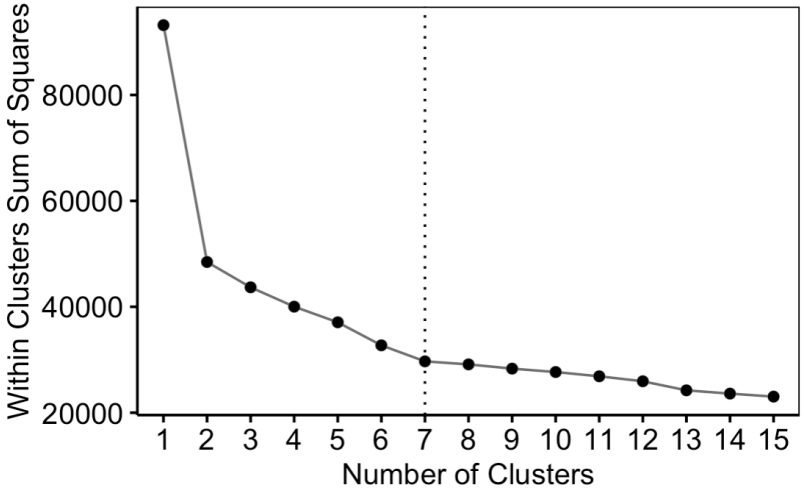

(b) SMI facilities

Figure 2.12: Plots of the within clusters sum of squares versus number of clusters (elbow method) for Ward's minimum variance linkage agglomerative hierarchical clustering of the major and SMI facilities.

- Restoration Time from LPV $\sim \text{Geometric}(1 - P^{R^L})$
- Restoration Time from HPV $\sim \text{Geometric}(1 - P^{R^H})$

Estimation of the Hidden Compliance States.

As presented in Table 2.2, high priority violations are relatively rare for both major and SMI facilities; only 1.62% and 0.98% of all inspections are resulting in HPV for major and

SMI facilities, respectively. To tackle the data limitation problem in our estimation, we initially combine the low priority and high priority violations as *non-compliance* (NC), and estimate the model on aggregated level with only two available compliance states (C, NC). The two state model is depicted in Figure 2.13. Upon categorizing the facilities into the appropriate number of clusters, we exploit a maximum likelihood approach to estimate the compliance transition parameters introduced in the Eq. 2.5. The probability of being in violation s periods after the last observed compliance (either compliant inspection or compliance restoration) can be computed by

$$q_n^{NC}(s) = \frac{\lambda_n}{\lambda_n + \mu_n}[1 - (1 - \lambda_n - \mu_n)^s]. \tag{2.5}$$

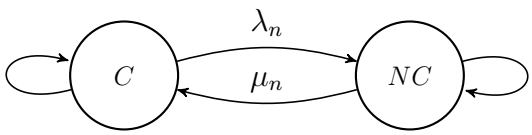

Figure 2.13: Two states transition probabilities of facility n if it is not inspected (NI) in a period.

Therefore, we need to estimate λ_n and μ_n to compute the $q_n^{NC}(s)$ for state s. Estimating λ_n and μ_n enables us to compute the probability of violation at each period. We further require to differentiate between the probability of being in low priority and high priority violation. To this end, we simply divide the $q_n^{NC}(s)$ by the relative average occurrence of LPVs and HPVs in each cluster.

Estimation of the Potential Environmental Harm.

We use the average past penalty paid by the facilities as the approximation of their potential environmental harm. Table 2.4 provides an overview of the past paid penalty by facilities. Note that the links between the violations and penalties are not available in the data set. After removing the outliers, we use the average of the highest penalties of each cluster (based on

the relative occurrence of the low and high priority violations) as the potential environmental harm associated with HPVs, and the average of the rest as the potential environmental harm of the LPVs.

Table 2.4: Average past paid penalty as the measure of environmental harm for EPA Region 2 facilities during 2002-2016.

	Major	SMI
Low priority violations	\$4,263	\$2,828
High priority violations	\$23,509	\$13,777

Overview of Parameter Estimation Results.

The estimated parameters for major and SMI facilities are presented in Table 2.5. These results are based on five clusters for major and seven clusters for SMI facilities.

Remark 4 *Note that the estimated parameters presented in Table 2.5 satisfy the Assumption 1, and can be used in simulation.*

We can also see that for all the clusters:

- *High priority violations are significantly less prevalent than low priority violations.*
- *The average restoration time from high priority violations is significantly higher than the average time of restoration from low priority ones. This can be translated as* $P^{R^H} > P^{R^L}$*. This is intuitive since HPVs are critical violations and may be naturally harder to resolve.*

Table 2.5: Estimated parameters for the EPA Region 2 facilities (Ward's minimum variance linkage agglomerative HCA).

(a) Major facilities

	Cluster number	1	2	3	4	5
Facilities	Number of facilities	57	269	146	91	270
Inspections	Total number of regular inspections	378	1,607	620	941	2,824
	Number of facilities with at least one regular inspection	57	262	133	91	268
	Average time between two regular inspections (weeks)	104.07	108.65	108.49	70.92	70.46
Violations	Percentage of LPV in regular inspections	9.00%	6.91%	6.77%	12.12%	11.12%
	Percentage of HPV in regular inspections	2.91%	2.80%	1.29%	1.28%	0.96%
	Percentage of all violations in regular inspections	11.91%	9.71%	8.06%	13.40%	12.08%
Environmental harm	Mean paid penalty for LPVs	\$3,669	\$2,553	\$3,010	\$8,083	\$6,523
	Mean paid penalty for HPVs	\$20,731	\$15,963	\$15,213	\$32,774	\$39,591
Compliance rates	λ	0.020	0.085	0.069	0.030	0.026
	μ	0.149	0.837	0.931	0.202	0.202
Restoration	Average restoration time from LPV (weeks)	14.21	11.50	9.88	9.81	11.18
	Average restoration time from HPV (weeks)	130.883	98.460	85.393	79.298	88.923
Restoration rates	P^{R^L}	0.9296	0.9130	0.8988	0.8981	0.9105
	P^{R^H}	0.9924	0.9898	0.9883	0.9874	0.9888

(b) SMI facilities

	Cluster number	6	7	8	9	10	11	12
Facilities	Number of facilities	1,203	394	548	913	334	567	364
Inspections	Total number of regular inspections	1,440	438	1,215	1,105	753	1,902	614
	Number of facilities with at least one regular inspection	856	225	440	695	279	519	261
	Average time between two regular inspections (weeks)	224.090	184.093	173.659	217.759	205.941	153.611	156.942
Violations	Percentage of LPV in regular inspections	0.56%	2.51%	6.83%	0.27%	1.59%	8.20%	3.42 %
	Percentage of HPV in regular inspections	0.56%	0.23%	2.47%	0.36%	0.40%	1.37%	0.16%
	Percentage of all violations in regular inspections	1.12%	2.74%	9.30%	0.63%	1.99%	9.57%	3.58%
Environmental harm	Mean paid penalty for LPVs	\$1,053	\$1,672	\$4,534	\$824	\$2,549	\$4,730	\$2,430
	Mean paid penalty for HPVs	\$7,806	\$6,173	\$19,164	\$7,562	\$11,917	\$20,005	\$10,600
Compliance rates	λ	0.001	0.010	0.016	0.001	0.015	0.089	0.032
	μ	0.194	0.980	0.218	0.204	0.928	0.904	0.674
Restoration	Average restoration time from LPV (weeks)	11.714	12.260	10.275	5.571	13.405	10.407	7.299
	Average restoration time from HPV (weeks)	58.411	89.429	39.148	23.464	199.143	94.685	104.286
Restoration rates	P^{R^L}	0.9146	0.9184	0.9027	0.8205	0.9254	0.9039	0.8630
	P^{R^H}	0.9829	0.9888	0.9745	0.9574	0.9950	0.9894	0.9904

2.6 Simulation

The objective of this section is to study the benefits of the Whittle's index proposed inspection strategy over other strategies suggested in academic literature and practice in reducing the *Average Expected Environmental Harm (cost)*. Our simulation is based on the following steps:

- We first implement the current's EPA practice as an indicator for the inspection capacities at each period and the main benchmark. Current EPA inspection policy as described in §2.5.2 suggests cyclic inspections with recommended intervals of 104 and 260 weeks for major and SMI facilities, respectively.

  We randomly initialize the states of the facilities at the beginning of the simulation (the states are randomly generated from 1 to 104 for major and 1 to 260 for SMI facilities). Then, we mark inspection for major and SMI facilities whenever their time since last inspection reaches 104 and 260 weeks, respectively. The number of facilities that reach their EPA recommend inspection cycle might be less than the periodic inspection capacity in some periods. In this case, we assign the remaining capacity to the inspections due on next period. On the other hand, if the number of required inspections exceeds the inspection capacity, we postpone the remaining inspections to the next period. We consider a long simulation length (l) to enhance the simulation results consistency (e.g., 1,560 weeks or 30 years).

- We then compute the Whittle's indices for the major and SMI facilities based on the parameters presented in Table 2.5. Note that we consider the same parameters for the facilities within the same cluster except for the environmental harms; we generate a random pair of LPV and HPV costs for each facility from the quartiles of the observed penalties in the analogous cluster to increase the variability. We set the maximum allowed time between two consecutive inspections (T) to be greater than the simulation length (l) to increase the flexibility of the inspection policies.

- We select the facilities based on the Whittle's index policy (and other benchmarks) in each period with respect to the EPA current capacity (M). We simulate the outcome of the inspections based on the estimated violation probability parameters of the aforementioned tables. If the simulated outcome of the inspection is LPV or HPV, we keep the facility away from further selection until the restoration is complete. The length of the restoration period is also randomly generated from the geometric distribution of the estimated restoration probabilities ($1-P^{R^L}$ and $1-P^{R^H}$) presented in Table 2.5.

- We compare the average cost per period for different policies over the length of simulation. We also record the number of inspections assigned to each cluster via each policy.

2.6.1 Scenarios for Inspection Capacity Allocation

In our simulation, we consider three different scenarios in fixing the inspection capacity per period:

- Equal workload is required for major and SMI facilities (1/1 workload scenario): In this scenario, we assume that all the facilities require the same resources for inspection regardless of their size. Current EPA inspection policy implies that, on average, 24.85% of the major and SMI get inspected annually, which we round down to 24 inspections per week. Thus, we set M = 24 for this scenario and keep it consistent across all the benchmark policies.

- Different workload is required for major and SMI facilities (1/0.8 workload scenario): In 1/0.8 workload scenario, we assume that SMI facilities require 80% of the workload needed to inspect major ones. This is aligned with the definition of synthetic minor facilities as the ones that (potentially) emit pollutant(s) at or above 80% of the major facilities [26].

- Separate capacities for major and SMI facilities: EPA current practice translates into 8 weekly inspections on major and 16 inspections on SMI facilities. Therefore, we can write the periodic capacity in the separate capacities scenario as $M = (M^{Maj}, M^{SMI}) = (8, 16)$.

2.6.2 Inspection Policies

Main Benchmark: Current EPA Practice (EPA 2/5 Policy).

Cyclic (periodic) inspection strategy is commonly studied in the operations management literature and adopted in practice. As an instance, [43] characterize conditions under which cyclic inspections can be superior to the random policy in advocating facilities' environmental compliance. Current U.S. CAA compliance monitoring strategy described in §2.5.2 is also a form of cyclic policy with intervals depending on facilities' emission size, we call this policy *EPA 2/5 policy*.

Whittle's Index Policy.

Whittle's index policy developed in §2.2 is our suggested policy.

Highest Expected Environmental Harm Selection Policy (EH Heuristic Policy).

An intuitive inspection strategy is selection based on the expected environmental harm of the facilities in each period. The expected environmental harm for facility n which is in state s at time t is given by $c_n^L q_n^L(s) + c_n^H q_n^H(s)$. This policy at each time t selects the facilities with the highest expected environmental harm according to the capacity.

Random Policy.

One of the inspection policies investigated in academic literature is random policy [43]. In the random policy, the regulator randomly selects facilities in each period to inspect without taking their characteristics and history into account.

2.6.3 Simulation Results and Policy Implications

Inspection Policies Performance under Different Capacity Allocation Scenarios.

We investigate the performance of each policy i under each inspection capacity allocation scenario. Our performance measure is reducing the average expected environmental harm (cost) compared to the current EPA 2/5 policy, which can be written as

$$\delta_i = \frac{cost^{EPA} - cost^i}{cost^{EPA}}.$$

Table 2.6 presents the improvement that each policy offers over the current EPA 2/5 policy. Figures 2.14, 2.15, and 2.16 also depict the percentage of the inspections assigned to each cluster along with the subsequent intervals between the consecutive inspections under these three inspection capacity allocation scenarios.

Table 2.6: Performance comparison of the inspection policies under different capacity allocation scenarios.

		$\delta_i\%$
1/1 workload	Whittle's index policy	$12.03\% \pm 0.06$
	EH heuristic policy	$10.74\% \pm 0.06$
	Random policy	$-0.79\% \pm 0.03$
1/0.8 workload	Whittle's index policy	$11.27\% \pm 0.05$
	EH heuristic policy	$9.77\% \pm 0.06$
	Random policy	$-0.66\% \pm 0.03$
Separate capacity per group	Whittle's index policy	$8.64\% \pm 0.05$
	EH heuristic policy	$7.23\% \pm 0.06$
	Random policy	$0.16\% \pm 0.04$

OBSERVATION 1 *As depicted in Table 2.6, the Whittle's index policy outperforms all the other policies under all the inspection capacity allocation scenarios. We can also see that the improvement is more significant for 1/1 workload, followed by 1/0.8 workload scenarios. This is due to the flexibility of these two scenarios that allow selection of the most harmful facilities regardless of their size.*

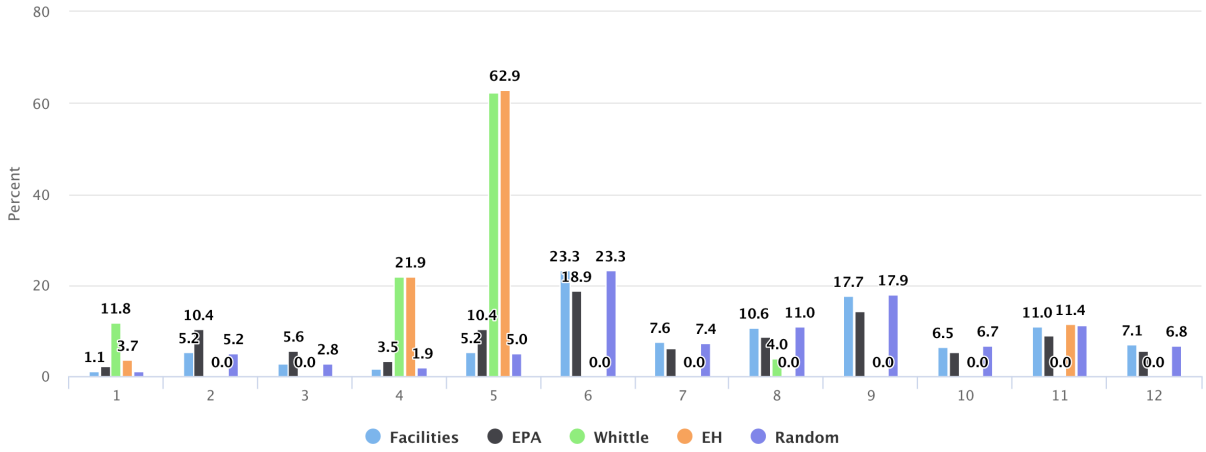

(a) Percentage of the inspections

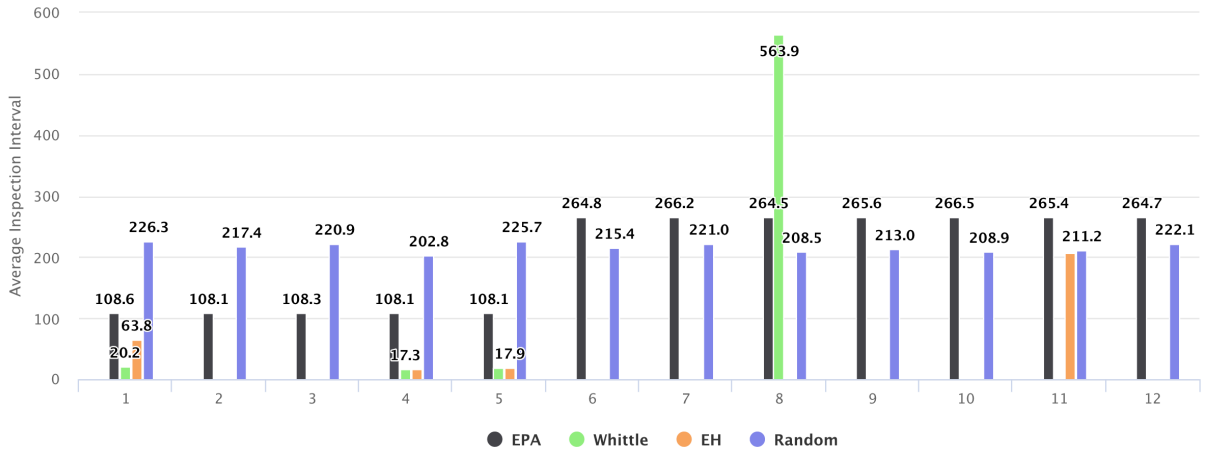

(b) Average interval between inspections

Figure 2.14: Percentage and average interval of the inspections assigned to each cluster of facilities-1/1 workload scenario.

OBSERVATION 2 *Figures 2.14, 2.15, and 2.16 show that in all the three capacity allocation scenarios Whittle's index policy focuses on inspecting facilities from clusters 5,4,1 and 8, respectively. These are the clusters with the highest violation rates and potential environmental harm as presented in Table 2.5.*

Performance of the Inspection Policies under Different Inspection Capacities.

We study the performance of inspection policies (§2.6.2) under a wide range of capacities ranging from $0.25M$ to $50M$ (M is the current EPA inspection capacity). All the simulations

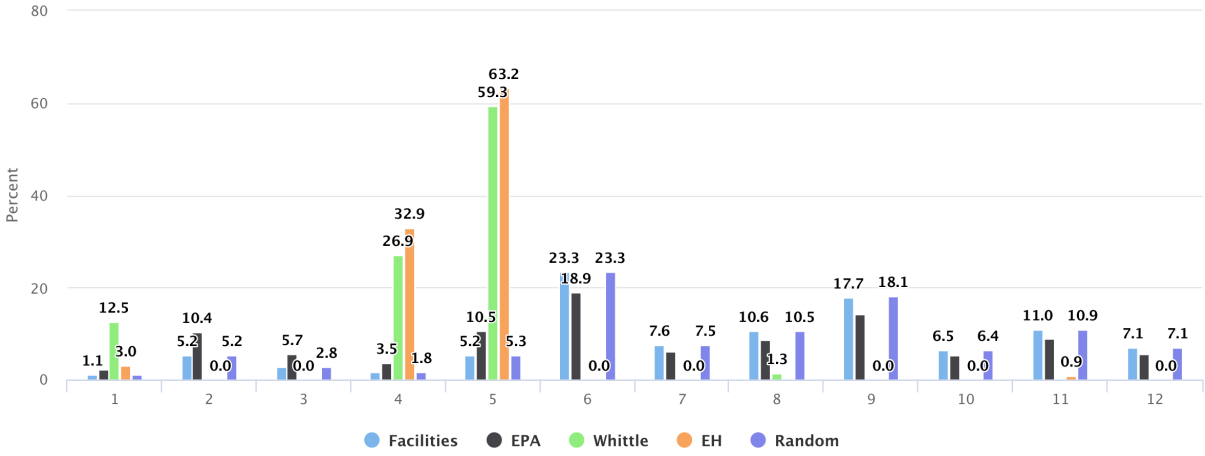

(a) Percentage of the inspections.

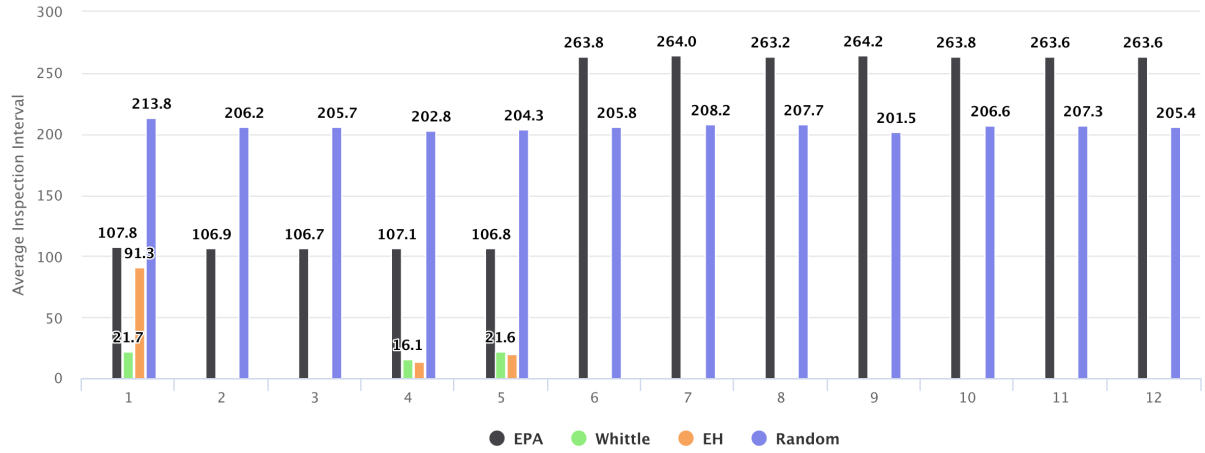

(b) Average interval between inspections

Figure 2.15: Percentage and average interval of the inspections assigned to each cluster of facilities-1/0.8 workload scenario.

have been conducted for the 1/0.8 workload scenario, which we believe is the closest to reality. For each policy i, along with the average environmental harm compared to the EPA 2/5 policy (δ_i), we also consider the marginal benefit of each inspection in reducing the environmental harm (δ'_i) defined as

$$\delta_i = \frac{cost^{EPA} - cost^i}{cost^{EPA}}, \qquad \delta'_i = \frac{\delta_i}{xM},$$

where $cost^{EPA}$, $cost^i$, x, and M represent the average cost of the EPA 2/5 policy,

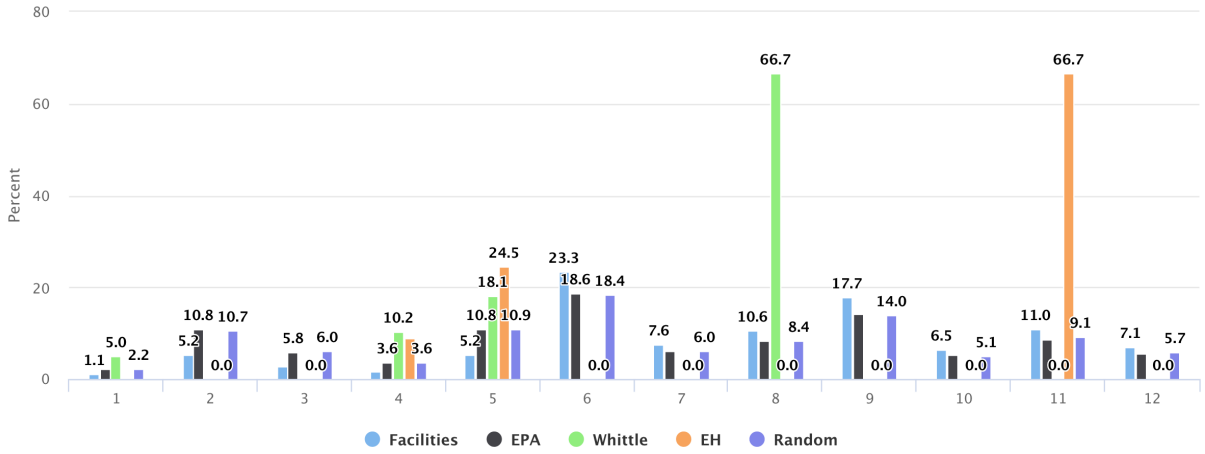

(a) Percentage of the inspections

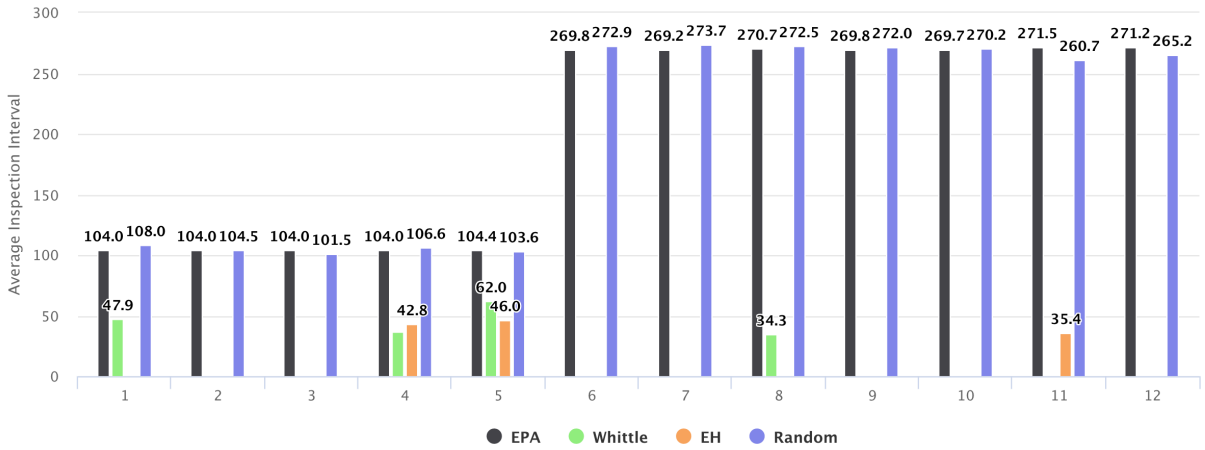

(b) Average interval between inspections

Figure 2.16: Percentage and average interval of the inspections assigned to each cluster of facilities-separate capacity per facility size scenario.

average cost of the policy i, current EPA inspection capacity, and the scaling coefficient of the capacity. Tables 2.7 and 2.8 provide an overview of the inspection policies performance and the subsequent capacity allocation among clusters for all the mentioned inspection policies.

Table 2.7: Performance comparison of inspection policies compared to the EPA 2/5 policy under different capacities-1/0.8 workload scenario.

Capacity	Inspection policy	$\delta_i\%$	δ_i'
$0.25M$	Whittle's index policy	$4.24\% \pm 0.04$	0.80%
	EH heuristic policy	$4.21\% \pm 0.04$	0.79%
	Random policy	$-0.26\% \pm 0.02$	-0.05%
$0.5M$	Whittle's index policy	$7.38\% \pm 0.05$	0.69%
	EH heuristic policy	$6.90\% \pm 0.05$	0.65%
	Random policy	$-0.50\% \pm 0.02$	-0.05%
$0.75M$	Whittle's index policy	$10.01\% \pm 0.05$	0.63%
	EH heuristic policy	$8.61\% \pm 0.05$	0.54%
	Random policy	$-0.52\% \pm 0.03$	-0.03%
M	Whittle's index policy	$11.27\% \pm 0.05$	0.53%
	EH heuristic policy	$9.77\% \pm 0.06$	0.46%
	Random policy	$-0.66\% \pm 0.03$	-0.03%
$1.25M$	Whittle's index policy	$12.27\% \pm 0.06$	0.46%
	EH heuristic policy	$10.04\% \pm 0.06$	0.38%
	Random policy	$-0.71\% \pm 0.04$	-0.03%
$1.5M$	Whittle's index policy	$13.08\% \pm 0.06$	0.41%
	EH heuristic policy	$11.04\% \pm 0.06$	0.35%
	Random policy	$-1.04\% \pm 0.04$	-0.03%
$1.75M$	Whittle's index policy	$14.33\% \pm 0.06$	0.38%
	EH heuristic policy	$12.24\% \pm 0.07$	0.33%
	Random policy	$-1.05\% \pm 0.04$	-0.03%
$2M$	Whittle's index policy	$15.28\% \pm 0.07$	0.36%
	EH heuristic policy	$12.25\% \pm 0.07$	0.29%
	Random policy	$-1.07\% \pm 0.05$	-0.03%
$5M$	Whittle's index policy	$24.64\% \pm 0.11$	0.23%
	EH heuristic policy	$22.55\% \pm 0.11$	0.21%
	Random policy	$-1.74\% \pm 0.08$	-0.02%
$10M$	Whittle's index policy	$36.25\% \pm 0.16$	0.17%
	EH heuristic policy	$31.95\% \pm 0.15$	0.15%
	Random policy	$-1.36\% \pm 0.11$	-0.01%
$20M$	Whittle's index policy	$48.97\% \pm 0.20$	0.11%
	EH heuristic policy	$47.26\% \pm 0.19$	0.11%
	Random policy	$2.20\% \pm 0.17$	0.01%
$50M$	Whittle's index policy	$55.87\% \pm 0.24$	0.05%
	EH heuristic policy	$54.96\% \pm 0.25$	0.05%
	Random policy	$18.00\% \pm 0.27$	0.02%

OBSERVATION 3 *As seen in Table 2.7, the Whittle's index policy outperforms EPA 2/5 policy and all the other benchmarks under all the considered capacities. Whittle's index policy leads to greater improvement in preventing environmental harm than the EPA 2/5 policy (δ_i) as capacity increases. We also observe that the marginal benefit of the Whittle's index suggested inspections (δ_i') increases as the capacity shrinks. This further accentuates*

the importance of our proposed Whittle's index policy considering the proposed budget cut for environmental inspections [16].

OBSERVATION 4 *Table 2.7 also shows that the highest expected environmental harm selection policy (EH heuristic policy) performs close to the Whittle's index policy under all the considered capacities. The highest expected environmental harm selection policy as a heuristic can be particularly of EPA's interest as a non-profit organization due to its high performance and ease of implementation.*

OBSERVATION 5 *According to Table 2.8, the Whittle's index policy progressively prioritizes the very high-risk clusters as we tighten the inspection capacity. For example, more inspections are assigned to cluster 5, which has the highest violation rates and potential environmental harm (see Table 2.5), as the capacity shrinks. On the other hand, more clusters are suggested for inspection by the Whittle's index policy as we increase the inspection capacity.*

2.7 Policy Implications and Managerial Insight

Simulation results presented in §2.6.3, demonstrate that the majority of the inspections are assigned to clusters 5 and 4 of major facilities under the current EPA capacity and the tighter ones. Comparative analyses on facilities' features (Table 2.1) show that *Prevention of Accidental Release/General Duty (CAAPARGD)* air program is applicable to 97.78% and 91.21% of the facilities within these two clusters, while it applies to less than 3.17% of the facilities in each of the other clusters. *CAAPARGD* is an air program related to facilities using substances that pose the greatest risk of harm from accidental releases. These facilities are required to have risk management programs that (i) asses the hazards of accidental release, (ii) safety preventive measures and maintenance, and (iii) emergency responses [27].

Table 2.8: Capacity allocation among clusters under different inspection policies-1/0.8 workload.

		Major							SMI				
Capacity	Cluster	1	2	3	4	5	6	7	8	9	10	11	12
	Facilities	1.11%	5.22%	2.83%	1.76%	5.24%	23.33%	7.64%	10.63%	17.71%	6.48%	11.00%	7.06%
	EPA 2/5 policy	3.38%	15.91%	8.63%	5.36%	15.88%	14.15%	4.63%	6.44%	10.74%	3.93%	6.67%	4.28%
$0.25M$	Whittle's index policy	13.73%	–	–	16.17%	70.10%	–	–	–	–	–	–	–
	EH heuristic policy	–	–	–	18.41%	81.59%	–	–	–	–	–	–	–
	Random policy	0.84%	4.86%	2.64%	1.81%	5.23%	24.80%	8.14%	9.75%	17.37%	6.36%	10.98%	7.22%
	EPA 2/5 policy	2.49%	11.76%	6.39%	4.04%	11.78%	17.74%	5.80%	8.13%	13.28%	4.93%	8.31%	5.34%
$0.5M$	Whittle's index policy	15.72%	–	–	23.56%	60.71%	–	–	–	–	–	–	–
	EH heuristic policy	–	–	–	16.37%	83.63%	–	–	–	–	–	–	–
	Random policy	1.05%	5.39%	2.85%	1.63%	5.06%	23.63%	8.01%	10.66%	17.60%	6.22%	10.69%	7.22%
	EPA 2/5 policy	2.26%	10.72%	5.80%	3.63%	10.72%	18.63%	6.17%	8.48%	14.11%	5.13%	8.73%	5.63%
$0.75M$	Whittle's index policy	14.68%	–	–	25.71%	59.62%	–	–	–	–	–	–	–
	EH heuristic policy	0.03%	–	–	31.97%	68%	–	–	–	–	–	–	–
	Random policy	1.07%	4.93%	2.65%	1.82%	4.88%	23.97%	7.36%	11.11%	17.72%	6.64%	11.07%	6.79%
	EPA 2/5 policy	2.19%	10.40%	5.66%	3.52%	10.46%	18.86%	6.17%	8.61%	14.29%	5.24%	8.89%	5.71%
M	Whittle's index policy	12.51%	–	–	26.92%	59.28%	–	–	1.29%	–	–	–	–
	EH heuristic policy	2.97%	–	–	32.93%	63.18%	–	–	–	–	–	0.91%	–
	Random policy	1.06%	5.20%	2.83%	1.79%	5.27%	23.31%	7.54%	10.52%	18.06%	6.45%	10.91%	7.06%
	EPA 2/5 policy	2.19%	10.31%	5.57%	3.47%	10.31%	19.00%	6.20%	8.69%	14.33%	5.25%	8.95%	5.73%
$1.25M$	Whittle's index policy	11.10%	0.76%	–	19.72%	59.61%	–	–	8.82%	–	–	–	–
	EH heuristic policy	1.87%	–	–	19.56%	46.70%	–	–	–	–	–	31.87%	–
	Random policy	0.97%	5.14%	2.74%	1.73%	5.33%	23.47%	7.68%	10.74%	18.06%	6.55%	10.63%	6.95%
	EPA 2/5 policy	2.19%	10.29%	5.57%	3.48%	10.28%	18.99%	6.22%	8.64%	14.39%	5.27%	8.94%	5.74%
$1.5M$	Whittle's index policy	11.06%	3.88%	–	21.14%	52.27%	–	–	11.65%	–	–	–	–
	EH heuristic policy	2.72%	–	–	16.90%	36.20%	–	–	–	–	–	44.18%	–
	Random policy	1.05%	5.09%	2.79%	1.70%	5.06%	23.49%	7.83%	10.66%	18.08%	6.51%	10.80%	6.92%
	EPA 2/5 policy	2.19%	10.31%	5.59%	3.49%	10.35%	19.01%	6.20%	8.63%	14.35%	5.25%	8.91%	5.72%
$1.75M$	Whittle's index policy	9.32%	10.01%	–	17.87%	46.63%	–	–	16.18%	–	–	–	–
	EH heuristic policy	2.08%	–	–	17.80%	36.61%	–	–	–	–	–	43.52%	–
	Random policy	1.04%	5.02%	2.74%	1.69%	5.10%	23.66%	7.54%	10.54%	17.85%	6.54%	11.14%	7.13%
	EPA 2/5 policy	2.19%	10.34%	5.59%	3.49%	10.36%	18.94%	6.21%	8.62%	14.37%	5.25%	8.91%	5.72%
$2M$	Whittle's index policy	8.08%	15.28%	–	16.33%	38.31%	–	–	22.01%	–	–	–	–
	EH heuristic policy	2.64%	–	–	16.63%	33.01%	–	–	–	–	–	47.73%	–
	Random policy	1.04%	5.21%	2.80%	1.73%	5.13%	23.40%	7.58%	10.74%	17.80%	6.55%	10.97%	7.05%
	EPA 2/5 policy	2.22%	10.46%	5.67%	3.54%	10.48%	18.86%	6.17%	8.58%	14.31%	5.24%	8.83%	5.65%
$5M$	Whittle's index policy	3.98%	18.47%	–	9.46%	21.88%	–	–	21.31%	–	–	24.90%	–
	EH heuristic policy	2.68%	14.49%	–	10.41%	24.14%	–	–	7.68%	–	–	40.60%	–
	Random policy	1.01%	5.02%	2.73%	1.76%	5.12%	23.75%	7.77%	10.67%	17.98%	6.53%	10.65%	7.01%
	EPA 2/5 policy	2.22%	10.47%	5.68%	3.54%	10.31%	18.86%	6.18%	8.60%	14.32%	5.24%	8.88%	5.70%
$10M$	Whittle's index policy	2.51%	18.87%	–	6.86%	17.97%	–	–	24.43%	–	–	29.36%	–
	EH heuristic policy	2.23%	13.38%	4.00%	9.34%	22.64%	–	–	14.72%	–	–	33.69%	–
	Random policy	0.99%	4.68%	2.71%	1.73%	5.06%	24.15%	7.89%	10.50%	18.25%	6.48%	10.37%	7.21%
	EPA 2/5 policy	2.28%	10.48%	5.68%	3.54%	10.40%	18.83%	6.17%	8.57%	14.28%	5.22%	8.86%	5.69%
$20M$	Whittle's index policy	1.92%	13.73%	3.58%	5.13%	17.21%	–	–	23.67%	–	–	34.76%	–
	EH heuristic policy	1.98%	11.13%	6.11%	6.33%	17.41%	–	–	23.05%	–	–	32.69%	1.30%
	Random policy	0.90%	4.26%	2.63%	1.63%	4.90%	24.74%	8.10%	10.40%	18.93%	6.46%	9.84%	7.22%
	EPA 2/5 policy	2.32%	10.95%	5.94%	3.70%	10.99%	19.62%	6.42%	8.93%	13.92%	4.55%	7.71%	4.95%
$50M$	Whittle's index policy	2.48%	5.39%	4.80%	4.99%	14.15%	5.57%	–	30.13%	4.74%	3.57%	15.83%	8.34%
	EH heuristic policy	2.60%	5.59%	4.70%	5.00%	15.00%	–	–	33.10%	–	7.55%	15.59%	10.87%
	Random policy	0.84%	3.20%	2.24%	1.54%	4.73%	26.55%	8.44%	10.50%	20.39%	6.19%	8.16%	7.22%

The other dominant feature for the cluster 5 and 4 facilities is *Chlorofluorocarbons (CFC) Tracking (CAACFC)* air program. This program is responsible for protecting the stratospheric ozone layer. The prevalence of this program is 98.89% and 96.70% in clusters 5 and 4, and less than 8.64% in each of the other clusters.

Among SMI facilities, cluster 8 is the only cluster suggested for inspection by the

Whittle's index policy under current EPA capacity. For significantly looser capacities, cluster 11 facilities are also recommended for inspections. These two clusters are the only SMI clusters with considerable *Title V (CAATVP)* facilities. Title V permit is required for major sources; SMI facilities are generally not required to obtain it unless they meet the particular conditions stated in [30]. 35.22% and 37.57% of clusters 8 and 11 facilities are subject to Title V permit, while this permit applies to less than 13.18% of facilities in each of the other SMI clusters.

2.8 Conclusion

In this work, we collaborated with EPA Region 2 and designed a facility-by-facility inspection strategy for Clean Air Act environmental monitoring program. We modeled the facility selection as a restless multiarmed bandit and proved the indexability of the subsequent model. We used a comprehensive data set of facilities' features and compliance history of EPA Region 2 to calibrate our model. Our simulation demonstrated that our index-based policy significantly outperforms the EPA current practice and other benchmarks in decreasing the environmental harm associated with the facilities' violations.

In our simulation, the Whittle's index policy assigned all the inspections to a few high-risk clusters under the current EPA's capacity suggesting that the differences among the facilities within each facility size (major and SMI) are substantial. Thus, the EPA current recommended inspection policy that treats all the facilities of the same emission size similarly requires critical modifications.

CHAPTER 3
MULTIPRODUCT DEMAND PREDICTION AND PRICE OPTIMIZATION USING NEURAL NETWORKS

3.1 Introduction

Electronics retail has turned into a highly competitive market with distinct features. On the one hand, many of the products share similar characteristics and can be regarded as substitutes. On the other hand, the products' prices are considerable enough that many customers actively look for the best deals. Posting the prices online by the retailers has also enabled the customers to easily track the prices of their desired products and make strategic purchasing decisions [8]. In other words, customers are not only able to pick the product with their target features among the pool of substitutes, but also can make an informed decision about which retailer to buy from. This flexibility highlights the importance of substitution and competition effects in the electronics retail industry, which have been barely addressed in traditional pricing systems.

This work aims to measure cross-price elasticities both within the product group and among competitor retailers, and design a multiproduct demand prediction and price optimization tool. We show how a consumer electronics retailer can benefit from the historical data to make a significantly more accurate demand prediction by taking the substitution and competition effects into account.

Estimating the cross-price elasticities would allow retailers to better understand the impact of price and assortment changes for products within a category on demand of other products in the product group. It would ultimately help them make multiproduct pricing decisions. Multiproduct demand prediction models typically lack either flexibility or interpretability. We propose a structure-imposed (structured) neural network framework that

balances these two and demonstrate how it can be used in price optimization.

3.2 Price Elasticity Definition

We first review the definition of elasticity and how it can be measured. There are two types of substitutes available for each product: similar products in the same category offered by the same retailer, and the identical product offered by competitor retailers. Throughout this chapter, we refer to the first set of products as "substitutable products", and the second as "competitors' products".

We deal with three types of elasticities: focal product elasticity, substitutable product cross-price elasticity, and competitor's product cross-price elasticity.

3.2.1 Focal Product Elasticity

Focal (own) product price elasticity show how the price of the product affect its own demand [34], and can be written as

$$e_f = \frac{\Delta Q_f}{\Delta P_f} = \frac{Q_f^2 - Q_f^1}{P_f^2 - P_f^1}. \tag{3.1}$$

Focal product elasticity is expected to have a negative sign as increasing the product price may decrease its demand.

3.2.2 Substitutable Product Cross-Price Elasticity

Substitutable product (similar products in the same category offered by the same retailer) cross-price elasticity is the change in the demand of the focal product versus change in the price of (each of the) substitutable products [34]. For a product with M substitutes within the product group, M substitutable cross-price elasticities can be defined. The substitutable product cross-price elasticity for a given focal product with respect to its $i-th$ substitutable

product is provided by

$$e_{sub_i} = \frac{\Delta Q_f}{\Delta P_{sub_i}} = \frac{Q_f^2 - Q_f^1}{P_{sub_i}^2 - P_{sub_i}^1}, \quad 1 \leq i \leq M. \tag{3.2}$$

Increasing the price of the substitute decreases its demand, which may turn to an increase in the demand of the focal product. Thus, the substitutable cross-price elasticity is expected to have positive sign.

3.2.3 Competitor's Product Cross-Price Elasticity

Competitor's product (identical product offered by competitor's retailer) cross-price elasticity refers to the change of the focal product's demand with respect to the change in the price of the same product offered by the competitor retailer. For a focal product offered through N other different retailers, there are N competitor cross-price elasticities.

$$e_{comp_i} = \frac{\Delta Q_f}{\Delta P_{comp_i}} = \frac{Q_f^2 - Q_f^1}{P_{comp_i}^2 - P_{comp_i}^1}, \quad 1 \leq i \leq N. \tag{3.3}$$

Competitor cross-price elasticity is also expected to have a positive sign.

3.3 Contributions to Literature and Practice

There are numerous works in the area of demand prediction and price optimization in the operations management literature. [19], [12], [62], and [55] study the pricing models in revenue management comprehensively. Particularly, [62] investigate in-depth the common demand models in the operations management literature, including linear demand function, log-linear demand function, constant elasticity demand function, and logit demand function. We select the linear demand function, one of the most widely used prediction models, as our baseline for comparison.

There is also significant academic research addressing the multiproduct pricing strategy. [59] focus on pricing the products within a product line by incorporating the cross-price

elasticities. [54] propose methods for the pricing of a set of interrelated products offered by a single retailer. [51] provide a theoretical framework for retail pricing and promotion policies of multiple product pricing. [11] investigate the optimal capacity levels and prices for two substitutable products in a single period problem. [60] study the multiproduct pricing problem through a non-parametric approach for a vehicle recommendation website. [45] consider dynamic pricing strategies for a firm that poses a fixed capacity that can be assigned to the production and delivery of multiple products.

Our work also focuses on the optimal product line pricing with one major difference: we use neural networks, one of the most powerful prediction techniques, for our elasticity and cross-price elasticity estimation. This makes our proposed approach more flexible and capable of accounting for more complicated relationships between the demand and its predictors.

There are several papers utilizing neural networks in demand prediction. For example, [17] use a robust neural network filter to one-day-ahead hourly electricity demand prediction for a local electricity utility. [6] predict domestic heat demand through neural networks. [64] forecast the cash demands in ATMs using clustering and neural networks. [1] predict urban residential water demand by neural network and time series models. [65] use deep neural networks to predict supply-demand for online car-hailing services. To the best of our knowledge, we are the first to utilize neural network-based demand prediction models in estimating the cross-price elasticities (both within product groups and across the competitors). In fact, our main contribution is designing a flexible yet interpretable neural network for multiproduct demand prediction and price optimization.

We are also aligned with the stream of research on developing pricing decision support tools for retailers. [61] design and implement a pricing support tool for clearance products. [15] develop and implement a decision support tool for a large apparel retailer's clearance period. They find the main predictors of the sales to be the previous sales, price elasticity, broken assortment effects, age of the article, and purchase quantity. [31] work with an

online retailer to optimize the pricing decision of flash sales and show how non-parametric models can be beneficial in pricing decision tools. We also benefit from collaborating with a consumer electronics retailer to estimate our demand model and measure the elasticities.

3.4 Demand Prediction Model

The first step in designing an efficient pricing decision tool is building an accurate demand prediction model. To estimate the substitutable and competitor cross-price elasticities, we use demand prediction models that incorporate focal, substitutable, and competitors' products' pricing features.

3.4.1 Our Partner Retailer and its Current Pricing Strategy

We utilize data of a consumer electronics retailer that we disguise its name. The in-store sales for this retailer account for 95% of its total revenue; therefore, we only focus on off-line sales. Our data covers the sales from January 2016 to June 2018.

The company currently divides the products into five categories with a different pricing strategy for each:

- Image setters: These are the most popular products. To position themselves as the price leader in the customers' minds, the retailer uses the lowest offered price in the market for such products.

- Standard products: These are the widely available yet less popular (than image setters) products. They are priced between minimum and maximum price of the competitors every day.

- Margin products: These are cheap products and it is unlikely that customers track or compare their prices while making purchasing decisions. The company prices them as high as possible.

- Dead articles: Products at the end of their life cycle, which are priced as low as possible to avoid further inventory costs.

We design a two-stage pricing system. In the first stage, we propose an interpretable structured neural network that addresses the substitution effects and show its advantage over the widely used linear regression model in accurate multiproduct demand prediction. In the second stage, we present the subsequent price optimization model.

3.4.2 Data Aggregation Level & Demand Prediction Components

We present the result of our analysis for televisions, one of the most popular product groups. This product group contains 49 different SKUs.

The retailer provided us with the sales SKU-day sales data in store level. We also have access to the daily inventory data of each SKUs and the promotions. We further pulled up data on the product's attributes for each SKU that we use for measuring the similarities in §3.4.3.

This retailer has three main competitor retailers in the country. We are provided with the prices offered by these competitors for each SKU on a daily basis. Note that although we focus on in-store sales, products' prices are available on the retailers' websites. Therefore, customers can easily check and compare the prices with no need to visit all the competitors' stores. Table 3.1 provides an overview of our data set.

Data	Level
Sales data	Store-SKU-Day
Price	Store-SKU-Day
Competitors' prices	SKU-Day
Promotions	Store-SKU-Type
Inventory	Store-SKU-Day
Product attributes	SKU

Table 3.1: Overview of the data provided by the retailer.

The first decision that we need to make for demand prediction is selecting the data

aggregation level. Although we have access to the SKU-Store level data, we decide to aggregate the data of the stores and predict the demand across them all for each SKU. Our decision rests on two reasons. First, the prices are unified over the stores. Additionally, the average of the sales is low for the majority of the SKUs, which makes predicting the sales at the store level inaccurate.

Then, we have to select features for the demand prediction model. Previous pricing papers divide the demand prediction predictors associated with the focal product to five categories: purchase quantity, age of the article, previous demand, broken assortment effect, and discount factor [15]. We follow the operations management literature and include the previous demand, age of the article, inventory level, and discount factor in our demand model. Our time series analyses show the impact of the day of the week and special days (holidays and special events) on the demand. We include dummy variables associated with days of the week and the major nation's holidays to take care of these effects. The auto-correlation analysis also suggests the importance of the one day and seven days lagged demand. Thus, we include the demand of the day before and the same day in the week before in our demand prediction model.

Another question that arises here is what features from the substitutable products and competitors to include in our model. The information from the substitutable products is internal, and we have all the factors described for the focal product available for substitutes as well. In contrast, the information about competitors is external, and we only have access to their daily prices. We use the lasso technique [41] as a variable selection model to select the pivotal variables among all the focal and substitutable products' features and the minimum competitor price. Following are the variables considered significant by lasso that we include in our demand prediction model:

- Previous demand: As described above, we incorporate the one day ($D_{f_i}^{t-1}$) and seven days ($D_{f_i}^{t-7}$) lagged demands in our prediction model. We expect both of them to have a positive relationship with the current demand.

- Focal product price ($P^t_{f_i}$): In our work, the price of the product is the second most important factor in determining the demand after the previous demands.

- Promotion rate ($d^t_{f_i}$): This relates to the special promotions being offered on the products. These promotions are advertised through flyers, internet or TV, and can potentially attract more customers. We subtract the promotion rate from one in our model to avoid using zero for products without promotion. For example, for a product with 20% promotion at time t, we consider $d^t_{f_i} = 1 - 0.2 = 0.8$.

- Inventory level ($I^{t-1}_{f_i}$): Rather than total availability across the stores, we use the percentage of the stores with sufficient inventory as inventory level. Note that we work with in-store sales, and we aggregated sales across the stores. Therefore, it is more intuitive to consider the percentage of the stores that have enough inventory to fulfill the local customers' demand rather than the total inventory over all the stores.

- Day of the week (W^t): These are dummy variables indicator of the day of the week. We include these variables since we observe a significant difference among the sales across the week. Especially, weekends have higher sales comparing to weekdays.

- Special day: A set of dummy variables associated with the major special events of the country (new year holidays, etc.). We use one dummy variable for each special day since each event may have a different effect on customers purchasing behavior.

- Price of the substitutable products ($P^t_{sub_{i,j}} \quad 1 \leq j \leq 3$): For the focal product f_i, we include the price of the top three substitutes. By definition of substitutable price elasticity in §3.2.2, we expect a positive relationship between the price of the substitutes and demand of the focal product.

- Substitutable products' promotions ($d^t_{sub_{i,j}} \quad 1 \leq j \leq 3$): We use the promotion rates of the substitutes (subtracted from one) along with their price in predicting the demand

of the focal products. We expect a positive relationship between the promotion of the substitutes and the demand of the focal products.

- Minimum competitors' price ($P^t_{comp_i}$): We use the minimum price of the competitor retailers in our model. According to the definition of the competitor cross-price elasticity provided in §3.2.3, the expected relationship between the minimum competitors' price and focal product's demand is positive.

3.4.3 Products' Similarity Analysis

One of the core steps to build a demand prediction model that incorporates the substitution effect is determining the substitution level among the products. We utilize data on products' attributes to quantify the similarity among the products in each product group. For example, we use the following features to measure the products' similarity for the TV group:

- Average price,
- Brand,
- Screen size,
- Screen resolution quality,
- Screen technology.

All the factors provided for (dis)similarity analysis (except average price) are categorical. We transform the average prices to the categorical variables as well (low, medium, high). Therefore, we need to use a similarity function that can effectively process categorical data.

There are several similarity measures developed for categorical data in computer science literature; for an in depth review of the measures see [13]. We adopt the Gower dissimilarity measure [38], which works based on the average of partial dissimilarities across individuals.

The Gower distance for a pair of products (i, j) with P features (f) can be written as

$$d(i,j) = \frac{1}{P}\Sigma_{f=1}^{P} d_{ij}^{f} \tag{3.4}$$

The partial dissimilarity for a categorical feature (f) equals zero only if observations f_i and f_j (the value of feature f for product i and j) have the same value, one otherwise. Gower dissimilarity measure is a score in $[0, 1]$ in which zero shows the complete similarity and one indicates the full dissimilarity. See [50] for details on how to compute some of the dissimilarity measures, including the Gower similarity score in R.

3.4.4 Linear Regression Model

The first model that we also set as the main baseline for our demand prediction model is linear regression. The structure of the linear regression for each focal product f_i based on the variables presented in §3.4.2 is

$$D_{f_i}^{t} = \beta_{f_i} X_{f_i}^{t} + \beta_{sub_i} X_{sub_i}^{t} + \beta_{comp_i} X_{comp_i}^{t} + c_i, \tag{3.5}$$

where $X_{f_i}^{t}$ denotes the components associated with the focal product and seasonality factors (previous demand, focal product price, promotion, inventory level, day of the week, and special day). $X_{sub_i}^{t}$ relates to the components of substitutable products, and $X_{comp_i}^{t}$ is the competitor related component. We can rewrite the Eq 3.5 as

$$D_{f_i}^{t} = \Sigma\beta_{f_i} X_{f_i}^{t} + \Sigma_{k=1}^{3}\beta_{sub_{ik}} P_{sub_{ik}}^{t} + \Sigma_{k=1}^{3}\beta_{sub_{ik}} d_{sub_{ik}}^{t} + \beta_{comp_i} P_{comp_i}^{t} + c_i. \tag{3.6}$$

We implement the linear regression model (Eq 3.6) on all 49 SKUs within the television product group. Table 3.2 depicts the results of the linear regression model for TVs' top 8 SKUs with the highest sales. These are the products with considerable daily sales and account for more than 51.47% of the total TV sales.

Table 3.2: Estimated elasticities for TVs bestsellers by linear regression (elasticities are recorded for 10% increase in the corresponding prices).

Product ID	Focal product elasticity	Substitutable products elasticity	Competitors'products elasticity
1	-13.02%	-0.56%	-5.03%
2	-8.24%	-0.39%	-2.86%
3	-16.36%	-0.76%	-6.56%
4	-12.76%	-0.59%	-4.47%
5	-9.87%	-0.43%	-3.54%
6	-13.46%	-0.56%	-4.82%
7	-10.89%	-0.49%	-3.99%
8	-17.03%	-0.68%	-6.56%

As we can see in Table 3.2, there are two major flaws in the results of the linear regression model:

- The substitutable products' elasticities have the same sign as the focal products' elasticities. This is illogical since, as we presented in §3.2.2, we expect substitutable products' cross-price elasticities to be positive.
- The competitors' cross-price elasticities come in the close magnitude with the focal products' price elasticities, which is unreasonable.

Estimated elasticities from the linear regression model contradict our intuition; this might be an indicator that the relationship between the substitutable (competitor) prices and the demand of the focal product is nonlinear. It may also indicate the inefficiency of linear regression in addressing the endogeneity of the focal and substitutable (competitor) prices. We alternatively suggest a structure-imposed neural network and show its ability to effectively estimate the focal and cross-price elasticities.

3.4.5 An Alternative Demand Prediction Model: Structure-Imposed Neural Network

We first start by providing the general framework of neural networks and their structures. We then present our proposed structure-imposed neural network and its mathematical structure.

General Framework of the Neural Network.

Neural networks are strong learning tools in the fields of statistics and Artificial Intelligence inspired by the brain's neurons. They have found wide applications in supervised and unsupervised learning [42]. Neural networks generally extract linear combinations of inputs to construct features, and then model the output by applying nonlinear functions on the derived features [40].

They consist of three main layers, and each layer may have one or more nodes:

- Input layer: The input layer relates to the external information (independent variables) provided to the model. No computation or transformation is performed in the input nodes; they solely pass the information to the hidden layer.

- Hidden layer: Hidden nodes within the hidden layer have no direct connection to the outside world. They do the computations and pass the information from input to the output layer.

- Output layer: Output nodes of the output layer are responsible for further computation and transferring the information from the network to outside. The outcome of the output layer is the target variable(s).

Figure 3.1 shows a simple design of a neural network and its layers. This network has two input nodes (1 and 2), three hidden nodes (3,4, and 5) and one output node (6).

The output of each node is the function of the weighted sum of the inputs, and weights are learned automatically by the network. The output of a node with P inputs can be written as

$$output_j = g(\theta_j + \Sigma_{i=1}^{P} w_{ij} x_i),$$

where $g(.)$ can be any function, including logistic, linear, and log-sigmoid.

Despite being a robust prediction tool, neural networks have always been criticized for the lack of interpretation. The complicated structure of the neural networks make the causal

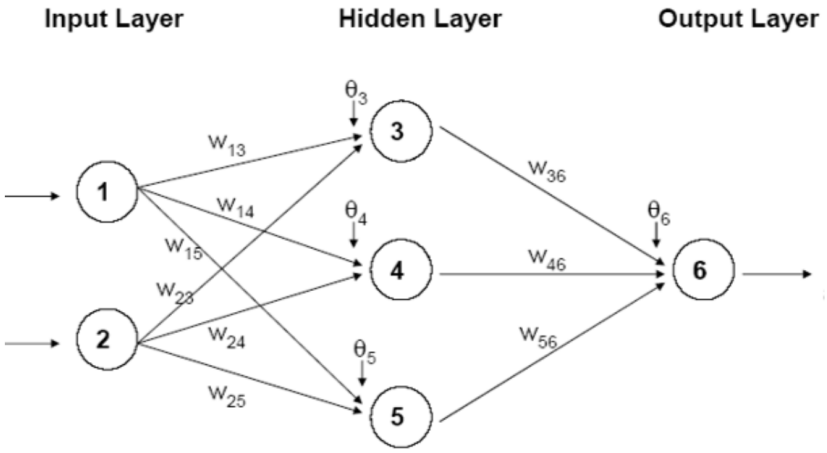

Figure 3.1: General structure of neural networks.

relationship of the inputs and outputs unclear [7]; therefore, they are particularly unsuitable for pricing settings. First, we cannot compute optimal prices without clearly expressing the relationship between price and demand by the demand prediction model. Second, industries may be hesitant to adopt uninterpretable pricing decision tools [31].

Structure-Imposed Neural Network.

To tackle the neural networks' interpretability issue, we propose a structure-imposed neural network and show how it can be effective in demand prediction.

Consistent with the §3.4.4, we divide our input into three categories for each focal product f_i at time t:

- Focal product associated components ($X^t_{f_i}$) consisting of focal product price ($P^t_{f_i}$), lagged demands, inventory level and seasonality factors, etc.
- Substitutable products associated components ($X^t_{sub_i}$) including $P^t_{sub_{i,j}}$ and $d^t_{sub_{i,j}}$ for $1 \leq j \leq 3$.
- Competitors associated components ($X^t_{comp_i}$). This can be simplified as $P^t_{comp_i}$ since we only include the minimum price of the competitors.

We also provide two nonlinear hidden layers in the structure. These layers are designed to represent the competition and substitution effects:

- Representative of substitutable products hidden layer (H_{sub}): This layer is connected to the substitutable and focal products' components. H_{sub} is supposed to estimate the substitutable cross-price elasticities. The weights and bias of this layer are denoted by W_{sub} and b_{sub}, respectively.

- Representative of competitors' products hidden layer (H_{comp}): It is connected to the competitors' and focal products' components. It aims to capture the competitor cross-price elasticities. The weights and bias are demonstrated by W_{comp} and b_{comp}, respectively.

Our output layer consists of a single node, and predicts the focal product demand ($D^t_{f_i}$). Weights and bias of the output layer are depicted by W_o and b_o. Figure 3.2 shows the schematic structure of our proposed neural network.

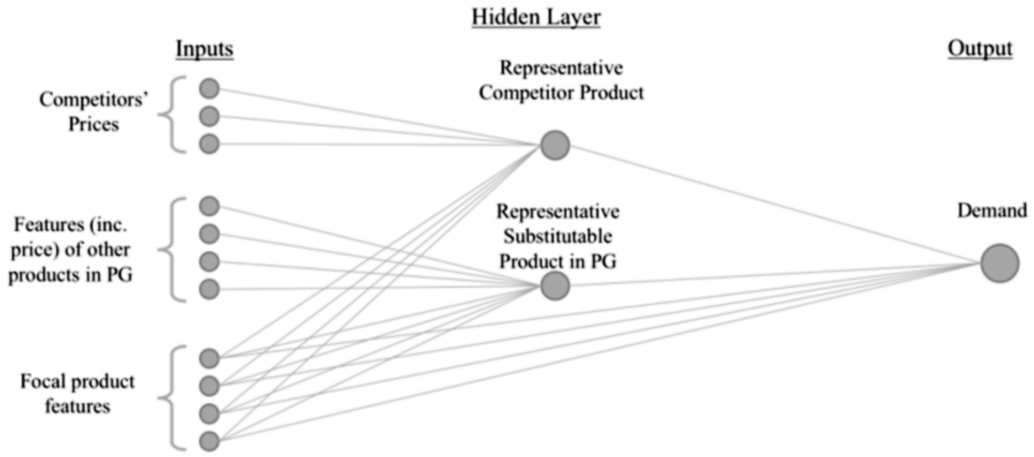

Figure 3.2: Schematic structure of the proposed neural network.

To implement our proposed neural network, we further require to select the activation function for the hidden layers. We tested different common choices (linear, logistic, log-sigmoid, radial), and use log-sigmoid activation function ($\sigma(\upsilon) = \frac{1}{1+e^{-\upsilon}}$) that showed best

performance in capturing the cross-price elasticities and demand prediction accuracy in our setting. Figure 3.3 presents the picture of our implemented neural network provided by MATLAB.

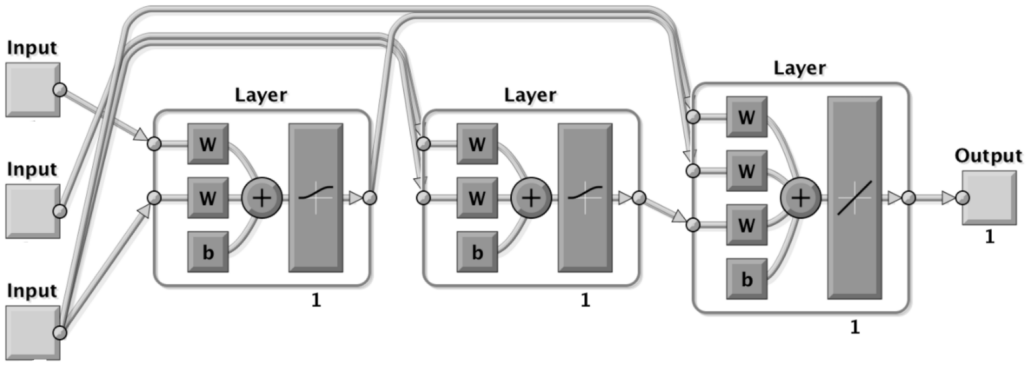

Figure 3.3: Structure of the proposed neural network implemented in MATLAB.

We train the network on the historical data, learn the weights of the connections, and subsequently estimate the elasticities and cross-price elasticities. Table 3.3 demonstrates the results of the estimated focal products' elasticities and cross-price elasticities for the TV bestsellers. The estimated elasticities from the structured neural network are more reasonable than the values estimated by linear regression (Table 3.2). The substitutable products' elasticities have expected signs. The competitor cross-price elasticities' magnitude is smaller compared to the values estimated by the linear regression, which is more reasonable.

Table 3.3: Estimated elasticities for TVs bestsellers by a structure-imposed neural network (elasticities are recorded for 10% increase in the corresponding prices).

Product ID	Focal product elasticity	Substitutable products elasticity	Competitors' products elasticity
1	-23.43%	1.86%	-1.26%
2	-19.48%	1.46%	-0.38%
3	-27.34%	2.17%	-0.59%
4	-28.42%	2.20%	-0.49%
5	-20.69%	1.78%	-0.72%
6	-22.94%	1.85%	-0.98%
7	-24.30%	2.02%	-0.99%
8	-33.44%	3.02%	-0.73%

Table 3.4 shows the comparison of the two models. While both linear regression and structured neural network are interpretable, structured neural network has significant advantages over the linear regression. It is more flexible than linear regression in estimating complicated patterns between the predictors and output. This makes it capable of estimating the cross-price elasticities with the expected sign and significantly improves the prediction accuracy compared to the linear regression. The structure-imposed neural network offers on average 23.91% improvement in the out of sample root mean squared error (RMSE).

Table 3.4: Comparison of the linear regression and structured neural network in elasticity estimation and prediction accuracy (average sales is 7).

	Linear regression	Structured neural network
Interpretability	✓	✓
Flexibility	✗	✓
Focal product elasticity	-12.70%	-25.00%
Substitutable cross-price elasticity	-0.56%	2.04%
Out of sample RMSE	5.48	4.17

To further show the strength of our proposed structure-imposed neural network, we also predict the demand for the same products with a full neural network with ten hidden layers (without any imposed structure). We observe that our proposed structured neural network has a prediction accuracy close to the full neural network (see Table 3.5). Thus, the imposed structure does not substantially decrease the prediction power of the original neural networks, while it solves their interpretability problem.

Besides the full neural network, we tested various other models and found the structure-imposed neural network to be superior to all; we present the result of the regression tree [41] as an instance. As we can see in Table 3.5, the structure-imposed neural network outperforms the prediction accuracy of regression trees.

Table 3.5: Prediction accuracy of various prediction models (average sales:7).

	Linear regression	Regression tree	Full neural network	Structured neural network
RMSE	5.48	4.61	4.03	4.17

Based on the mentioned points, we use our proposed structure-imposed neural network among all the discussed models in our pricing decision tool. In what follows, we provide our subsequent price optimization approach for finding the optimal prices for each product.

3.5 Price Optimization

After predicting the demands, we need to optimize the prices to maximize the daily revenue (R^t) for each category. Our objective function in this stage can be written as

$$\begin{aligned} &\max R^t = \Sigma_{i=1}^{M} D_{f_i}^t P_{f_i}^t, \\ &P_i^{min} \leq P_{f_i}^t \leq P_i^{max}, \end{aligned} \tag{3.7}$$

where M, $D_{f_i}^t$, and $P_{f_i}^t$ denote the number of products in the category, demand and price of the $i-th$ product at time t, respectively. The allowed price of each product ($P_{f_i}^t$) is also constrained between a minimum and maximum value (P_i^{min} and P_i^{max}), which are set by the retailer.

In order to solve the Eq 3.7 and finding the optimal prices, we need to explicitly write the relationship between the demand predicted by structure-imposed neural network and offered prices. Thus, we study the mathematical structure of our proposed demand model next.

3.5.1 Mathematical Representation of the structure-imposed Neural Network

Following the structure presented in §3.4.5, we can write the structure of the hidden and output layers as

$$H_{sub} = \sigma(b_{sub} + W_{sub}[X^t_{sub_i}; X^t_{f_i}]), \tag{3.8a}$$

$$H_{comp} = \sigma(b_{comp} + W_{comp}[X^t_{comp_i}; X^t_{f_i}]), \tag{3.8b}$$

$$D^t_{f_i} = b_o + W_o[H_{sub}; H_{comp}; X^t_{f_i}]. \tag{3.8c}$$

By substituting the value of the fixed inputs (the predetermined independent variables), the Eq 3.8 can be rewritten as

$$H_{sub} = \sigma(c_{sub} + \sum_{k=1}^{3} w_{sub_{ik}} P^t_{sub_{ik}} + w_{sub_{f_i}} P^t_{f_i}), \tag{3.9a}$$

$$H_{comp} = \sigma(c_{comp} + w_{comp_{f_i}} P^t_{f_i}), \tag{3.9b}$$

$$D^t_{f_i} = b_o + w_{o,sub} H_{sub} + w_{o,comp} H_{comp} + (c_f + w_{o,f} P^t_{f_i}). \tag{3.9c}$$

The mathematical structure of the demand can be simplified as

$$D^t_{f_i} = c + \frac{w_{o,sub}}{1 + e^{-(c_{sub} + \sum_{k=1}^{3} w_{sub_{ik}} P^t_{sub_{ik}} + w_{sub_{f_i}} P^t_{f_i})}} + \frac{w_{o,comp}}{1 + e^{-(c_{comp} + w_{comp_{f_i}} P^t_{f_i})}} + w_{o,f} P^t_{f_i}. \tag{3.10}$$

3.5.2 Price Optimization Tool

Combining the Eq. 3.7 and Eq.3.10, the revenue optimization function based on the structure-imposed neural network can be expressed as

$$
\begin{aligned}
Max \quad R^t &= \Sigma_{i=1}^{M} D_{f_i}^t P_{f_i}^t, \\
&= \Sigma_{i=1}^{M} (c + \frac{w_{o,sub}}{1 + e^{-(c_{sub} + \sum_{k=1}^{3} w_{sub_{ik}} P_{sub_{ik}}^t + w_{sub_{f_i}} P_{f_i}^t)}} + \frac{w_{o,comp}}{1 + e^{-(c_{comp} + w_{comp_{f_i}} P_{f_i}^t)}} \\
&+ w_{o,f} P_{f_i}^t) P_{f_i}^t, \\
P_i^{min} &\leq P_{f_i}^t \leq P_i^{max}.
\end{aligned} \tag{3.11}
$$

Figure 3.4 demonstrates multiple shapes of the revenue function for single product pricing (all the substitutable products' prices remained constant). As we can see in these plots, finding the optimal price even for a single product case is challenging, and the revenue function may be ill-behaved.

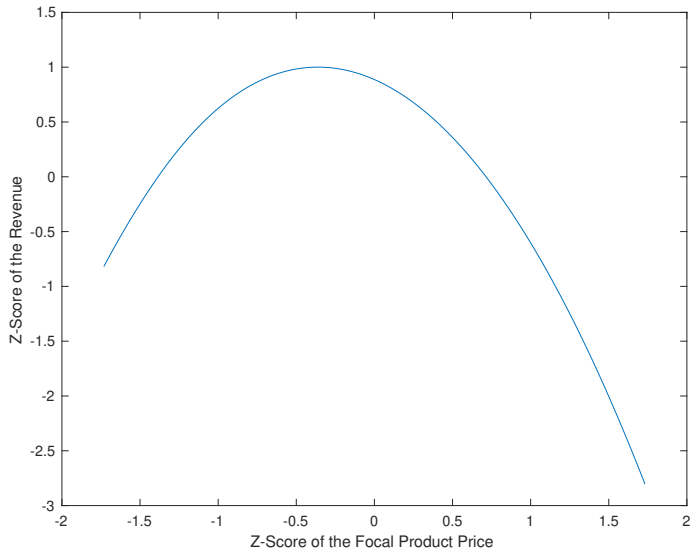

(a) Case I

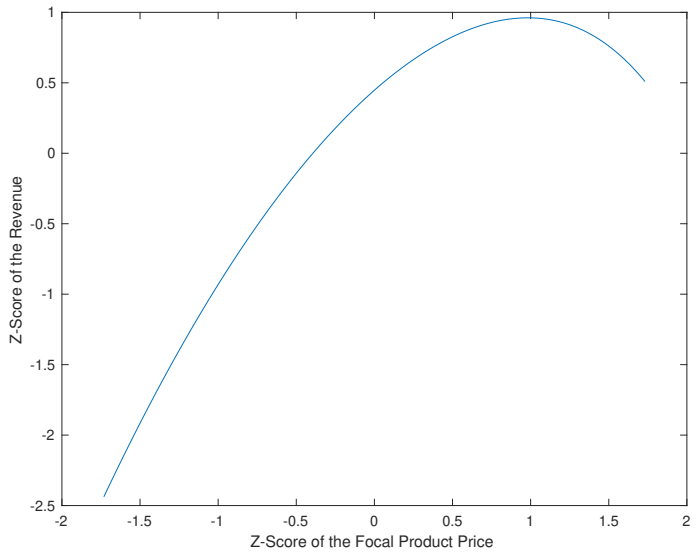

(b) Case II

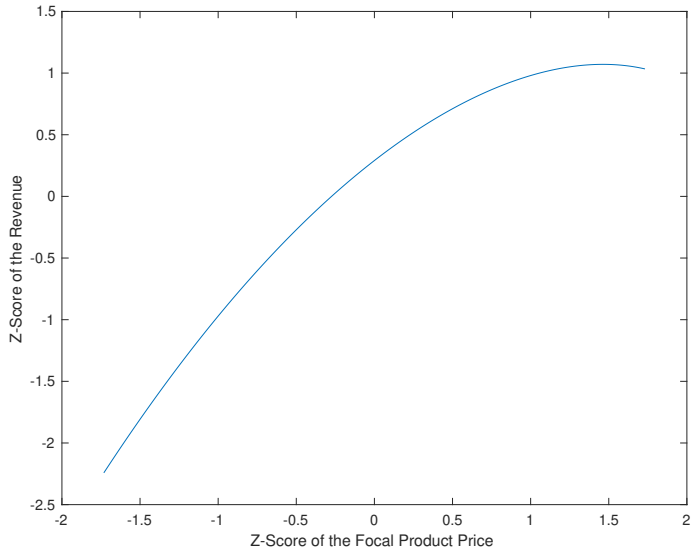

(c) Case III

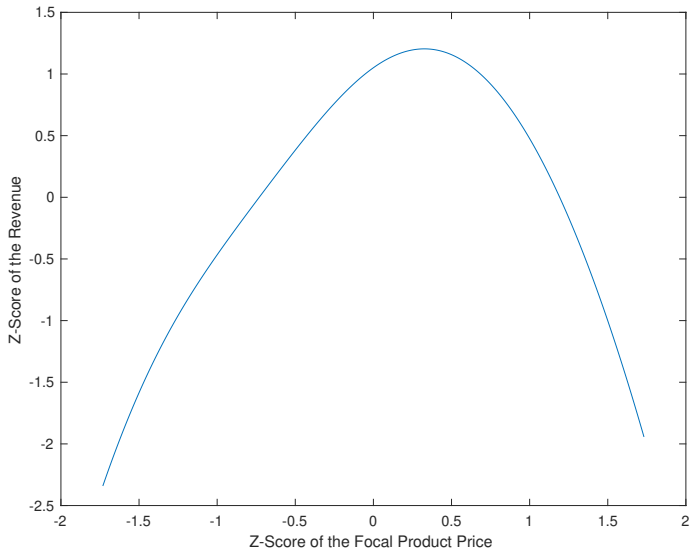

(d) Case IV

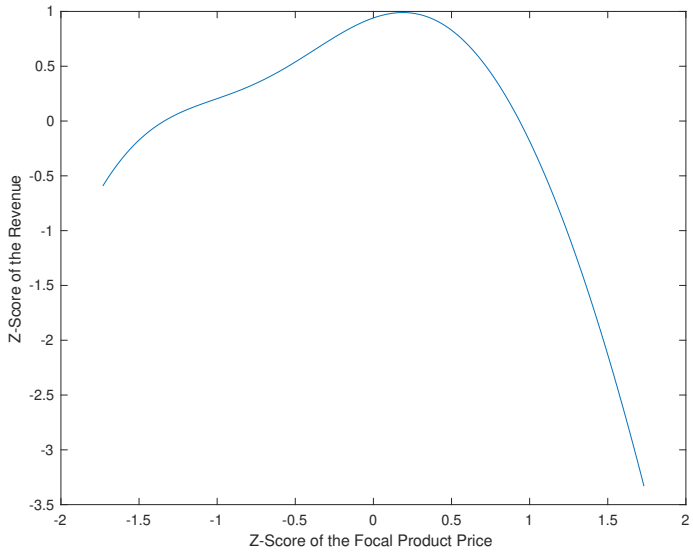

(e) Case V

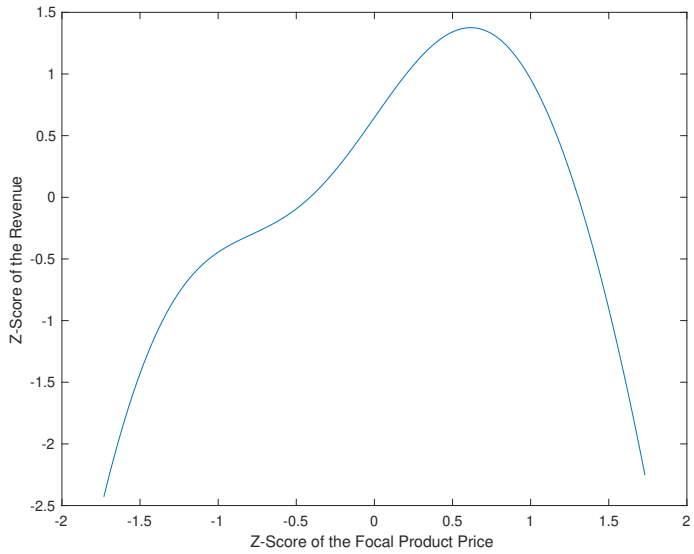

(f) Case VI

Figure 3.4: Plots of the z-score of the focal product price versus its own revenue function-single product pricing scenario.

For solving the constrained multiproduct price optimization, we use the *fmincon* command of MATLAB [47]. Constraints are the upper and lower bounds of the price of each product (minimum and max allowed price determined by the retailer). fmincon is designed to solve the constrained nonlinear multi-variable optimization problems. It works using sequential quadratic programming (SQP).

Sequential quadratic programming (SQP) is an iterative method for constrained nonlinear optimization and solves a sequence of quadratic programming optimization subproblems at each iteration [33]. The Hessian at each iteration is approximated by Broyden-Fletcher-Goldfarb-Shanno (BFGS) algorithm [58, 57]. Note that although we run the optimization problem with different initializations to avoid local maxima solutions as much as possible, finding an optimal solution is not guaranteed in this method.

3.5.3 Impact of the Proposed Pricing Decision Tool on the Retailer Revenue

To show the efficiency of our proposed pricing decision tool, we first compare the total actual revenue of the retailer for TV high sellers with the predicted revenue by the structure-imposed neural network for January 2016 to June 2018. The actual revenue of the retailer for these 8 products is computed by

$$R_{Actual} = \Sigma_{i=1}^{8} \Sigma_{t=1}^{T} D_{i(Actual)}^{t} P_{i(Actual)}^{t},$$

where $D_{i(Actual)}^{t}$, and $P_{i(Actual)}^{t}$ denote the actual demand and price of the product i at time t.

The predicted revenue of the retailer for these 8 products is

$$R_{Pred} = \Sigma_{i=1}^{8} \Sigma_{t=1}^{T} D_{i(Pred)}^{t} P_{i(Actual)}^{t},$$

where $P_{i(Actual)}^{t}$ and $D_{i(pred)}^{t}$ represent the actual price offered by the retailer and analogous predicted demand by our structure-imposed neural network for the product i at time t.

The revenue prediction error by our proposed structured neural network can be written as

$$\delta_1 = \frac{R^{Pred} - R^{Actual}}{R^{Actual}}$$

OBSERVATION 6 *The error of the predicted revenue (δ_1) is 14.52% for the TV bestsellers during the considered period.*

Then, we compare the predicted revenue with the optimal revenue derived by our pricing tool. The optimal total revenue of our suggested pricing tool (structure-imposed neural network demand prediction model and its subsequent optimization technique) can be expressed by

$$R_{Opt} = \Sigma_{i=1}^{8} \Sigma_{t=1}^{T} D_{i(Opt)}^{t} P_{i(Opt)}^{t},$$

$P_{i(Opt)}^{t}$ and $D_{i(Opt)}^{t}$ correspond to the optimal price and its analogous demand predicted by the structured neural network-based pricing tool.

The improvement in the revenue provided by our pricing tool is

$$\delta_2 = \frac{R^{Opt} - R^{Pred}}{R^{Pred}}$$

OBSERVATION 7 *Our analysis predicts the aggregated improvement of* 6.92% *in the total revenue for the TV bestsellers for the mentioned time frame.*

3.6 Conclusion

In this chapter, we investigated the application of neural networks in multiproduct pricing. We believe our work has two main contributions to the revenue management literature. Firstly, we developed an interpretable structure-imposed neural network for multiproduct demand prediction. The imposed structure resolves the interpretability problem of the neural networks that made them impractical for pricing problems. Secondly, we included cross-price elasticities in the demand prediction model. We formulated the mathematical structure of the subsequent demand and revenue function and provided the optimization technique.

Our structure-imposed neural network provided promising results in estimating the cross-price elasticities. It also improved the out of sample root mean squared error for the demand prediction by on average 23.91%. Our analyses for different product groups showed that high price product groups benefit most from our pricing tool. This is intuitive as customers tend to make more comparisons both within-category and across competitors to purchase expensive products, highlighting substitution and competition effects.

CHAPTER 4
CONCLUDING REMARKS

In this thesis, we demonstrated how analytics could support operational decision making in both nonprofit and for-profit settings.

In nonprofit operations, we proposed a priority-based inspection strategy to assist the environmental regulators such as the U.S. EPA in their targeting process for environmental monitoring. We modeled the facility selection for environmental inspection as a restless multiarmed bandit and proved our model's indexability implying that our suggested policy is asymptotically optimal as the number of facilities goes to infinity (for a fixed capacity). In our general modeling framework, we assumed that facilities could be in compliance, low priority violations, or high priority violations with respect to the environmental regulations at each point of time. Upon conducting an inspection, noncompliant facilities had to enter the respective *restoration* states and remain there until full compliance was achieved. The transition rates among all the states (compliance and restoration) were governed by rates depending on facilities' features.

We further calibrated our model based on the Clean Air Act inspections data of the EPA Region 2. We clustered the facilities based on their static characteristics (demographic, location, type of industry, emission programs, and type of ownership) and estimated the transition rates for each cluster separately. The estimated parameters were used in our comprehensive simulations to compare the performance of our proposed Whittle's index policy with current EPA inspection strategy and other benchmarks. We also addressed two extensions of our model, including the inspections with heterogeneous costs and the possibility of disaster in the facilities.

Our experience in working with a nonprofit organization (Environmental Protection Agency) has revealed a big gap between policy design research (environmental compliance

research in our case) and data science. There are many barely utilized data sets that can be beneficial in supporting the environmental regulators' decisions that remained unused. This happens because the environmental scientists are not familiar with the analytical methods, and data scientists are not aware of these research opportunities.

Our work opens new avenues in applying analytical techniques in environmental compliance strategy design. Future research can investigate the effect of our suggested policy on facilities' self-reporting of the violation. Considering the effect of self and peer learning among the facilities on optimal inspection strategy design is another potential research stream. For example, we assumed that the facilities' compliance rates are exogenous and independent of the regulator inspection strategy, while the regulator inspection strategy might induce strategic behavior in facilities over time.

In the second part of the thesis, we presented our work in partnership with a consumer electronics retailer. More and more data are becoming available in retail operations, and customers have the chance to compare the prices and make more informed purchasing decisions. Specifically, customers are able to compare the prices more frequently to decide what product to buy within a product category and which seller to buy from. This introduces substitution within the product category and among competitors in the market.

We demonstrated how the retailer could incorporate these substitution effects in their multiproduct pricing decision making. Due to the complicated (nonlinear) nature of the substitutable and competitors' products' prices with the focal product's demand, traditional linear models cannot predict the substitutable and competitor elasticities correctly. We introduced structure-imposed neural network as an alternative for the linear regression model. We showed that our neural network is not only able to predict the sign and magnitude of the substitutable and competitor price elasticities reasonably, but also significantly improves the accuracy of the demand prediction. We further demonstrated how we can use the structured neural network demand prediction function in multiproduct price optimization.

This chapter can be extended by addressing the pricing game between the retailer and

its competitors. This is an influential research direction since retailers usually follow their competitors and react to each other offered prices. Addressing the endogeneity between the focal product price and substitutable products' prices is also another essential research stream.

Appendices

APPENDIX A

PROOFS OF THE CHAPTER 2

Proof of Lemma 1.

We drop the facility index n for notation simplicity. Clearly, for any given facility, when the environmental costs and the transition probabilities are fixed, the optimal long-run average cost $\gamma(v)$ is increasing in v.

For $s = T$, since we assume the time between two consecutive inspections cannot exceed T, we must take the inspection action. Therefore, we have

$$h(T, v) = -\gamma(v) + \mathbf{c}^\top \mathbf{q}(T) + \mathbf{g}(v)^\top \mathbf{q}(T) + v.$$

Let $\tilde{h}(t, v) := h(t, v) - \mathbf{g}(v)^\top \mathbf{q}(t-1) - v$. We want to prove that $\tilde{h}(T, v) := h(T, v) - \mathbf{g}(v)^\top \mathbf{q}(T-1) - v$ is decreasing in v. This quantity can be written as

$$\begin{aligned}
\tilde{h}(T, v) &:= h(T, v) - \mathbf{g}(v)^\top \mathbf{q}(T-1) - v \\
&= -\gamma(v) + \mathbf{c}^\top \mathbf{q}(T) + \mathbf{g}(v)^\top \mathbf{q}(T) + v - \mathbf{g}(v)^\top \mathbf{q}(T-1) - v \\
&= -\gamma(v) + \mathbf{c}^\top \mathbf{q}(T) + \mathbf{g}(v)^\top (\mathbf{q}(T) - \mathbf{q}(T-1)).
\end{aligned}$$

Note that $-\gamma(v)$ is decreasing in v since $\gamma(v)$ is increasing in v. The second term, $\mathbf{c}^\top \mathbf{q}(T)$ is independent of v. The last term, $\mathbf{g}(v)^\top (\mathbf{q}(T) - \mathbf{q}(T-1))$, is equal to

$$\mathbf{g}(v)^\top (\mathbf{q}(T) - \mathbf{q}(T-1)) = h(R^{LPV})(q^L(T) - q^L(T-1)) + h(R^{HPV})(q^H(T) - q^H(T-1)),$$

according to the definition of the vector $\mathbf{g}(v)$. By the Bellman equation Eq (2.2), both $h(R^{LPV})$ and $h(R^{HPV})$ are negative and decreasing in v. By Assumption 1, $q^L(T) \geq q^L(T-1)$, $q^H(T) \geq q^H(T-1)$. Thus, the last term is also decreasing in v. In sum, we

proved that $\tilde{h}(T, v)$ is decreasing in v.

Now, we prove the induction step. Assuming $\tilde{h}(s+1, v)$ is decreasing in v, we want to prove that $\tilde{h}(s, v)$ is also decreasing in v. By the Bellman's equation (2.1a), we have

$$\begin{aligned} h(s, v) &= -\gamma(v) + \mathbf{c}^\top \mathbf{q}(s) + \min\{\mathbf{g}(v)^\top \mathbf{q}(s) + v, h(s+1)\} \\ &= -\gamma(v) + \mathbf{c}^\top \mathbf{q}(s) + \min\{0, \tilde{h}(s+1)\} + \mathbf{g}(v)^\top \mathbf{q}(s) + v. \end{aligned}$$

Thus, we have

$$\begin{aligned} \tilde{h}(s, v) :&= h(s, v) - \mathbf{g}(v)^\top \mathbf{q}(s-1) - v \\ &= \Big(-\gamma(v) + \mathbf{c}^\top \mathbf{q}(s) + \min\{0, \tilde{h}(s+1)\} + \mathbf{g}(v)^\top \mathbf{q}(s) + v\Big) - \mathbf{g}(v)^\top \mathbf{q}(s-1) - v \\ &= \Big(-\gamma(v) + \mathbf{c}^\top \mathbf{q}(s) + \min\{0, \tilde{h}(s+1)\}\Big) + \mathbf{g}(v)^\top \big(\mathbf{q}(s) - \mathbf{q}(s-1)\big) \end{aligned}$$

We now analyze the monotonicity of each term above.

The first term, $\Big(-\gamma(v) + \mathbf{c}^\top \mathbf{q}(s) + \min\{0, \tilde{h}(s+1)\}\Big)$, is decreasing in v, since $-\gamma(v)$ is decreasing in v and $\tilde{h}(s+1, v)$ is decreasing in v by the induction assumption. The second term, $\mathbf{g}(v)^\top \big(\mathbf{q}(s) - \mathbf{q}(s-1)\big)$, is equal to

$$\mathbf{g}(v)^\top \big(\mathbf{q}(s) - \mathbf{q}(s-1)\big) = h(R^{LPV})(q^L(s) - q^L(s-1)) + h(R^{HPV})(q^H(s) - q^H(s-1)).$$

Recall that $h(R^{LPV})$ and $h(R^{HPV})$ are negative and decreasing in v. By Assumption 1, $q^L(s) \geq q^L(s-1)$, $q^H(s) \geq q^H(s-1)$, so the second term is also decreasing in v. Therefore, we conclude that $\tilde{h}(s, v)$ is also decreasing in v. This completes the proof. ■

Proof of Theorem 1. We write $h_n(s, v) := h_n(s)$ to emphasize that it is dependent on the activation fee v. The Bellman's equation (2.1) can be rewritten as

$$h_n(s, v) = -\gamma_n(v) + \mathbf{c}_n^\top \mathbf{q}_n(s) + \min\{\mathbf{g}_n(v)^\top \mathbf{q}_n(s) + v, h_n(s+1)\}.$$

This implies that the optimal decision is to inspect if and only if $\tilde{h}_n(s+1, v) = h_n(s+$

$1, v) - \mathbf{g}_n(v)^\top \mathbf{q}_n(s) - v$ is positive.

Now, let us increase the activation cost from v to v'. Consider a state $\bar{s} \in \{1, \cdots, T-1\}$ for which no inspection is optimal, i.e., $\bar{s} \in \mathcal{S}_n(v)$. It holds that $\tilde{h}_n(\bar{s}+1, v) \leq 0$. By Lemma 1, we have $\tilde{h}_n(s+1, v') \leq \tilde{h}_n(s+1, v) \leq 0$. Thus, we $\bar{s} \in \mathcal{S}_n(v')$, which implies $\mathcal{S}_n(v) \subset \mathcal{S}_n(v')$. This completes the proof of indexability.

■

Proof of Lemma 2 We drop the facility index n for notation simplicity once again. Again, for any given facility, when the environmental costs and the transition probabilities are fixed, the optimal long-run average cost $\gamma(v)$ is increasing in v.

For $s = T$, we have

$$h(T, v) \;=\; -\gamma(v) + \mathbf{c}^\top \mathbf{q}(T) + \mathbf{g}(v)^\top \mathbf{q}(T) + q^D(T) h(D) + v.$$

Let $\tilde{h}(t, v) \;=\; (1 - q^D(t-1)) h(t, v) - \mathbf{g}(v)^\top \mathbf{q}(t-1) - v$. We want to prove that $\tilde{h}(T, v) := (1 - q^D(T-1)) h(T, v) - \mathbf{g}(v)^\top \mathbf{q}(T-1) - v$ is decreasing in v. This quantity can be written as

$$\begin{aligned}
\tilde{h}(T, v) &:= (1 - q^D(T-1)) h(T, v) - \mathbf{g}(v)^\top \mathbf{q}(T-1) - v \\
&= (1 - q^D(T-1)) \Big(-\gamma(v) + \mathbf{c}^\top \mathbf{q}(T) + \mathbf{g}(v)^\top \mathbf{q}(T) + q^D(T) h(D) + v \Big) \\
&\quad - \mathbf{g}(v)^\top \mathbf{q}(T-1) - v \\
&= (1 - q^D(T-1)) \Big(-\gamma(v) + \mathbf{c}^\top \mathbf{q}(T) + q^D(T) h(D) \Big) \\
&\quad + \Big((1 - q^D(T-1)) \mathbf{g}(v)^\top \mathbf{q}(T) - \mathbf{g}(v)^\top \mathbf{q}(T-1) \Big) - q^D(T-1) v
\end{aligned}$$

Note that in $(1 - q^D(T-1)) \Big(-\gamma(v) + \mathbf{c}^\top \mathbf{q}(T) + q^D(T) h(D) \Big)$, $-\gamma(v)$ is decreasing in v since $\gamma(v)$ is increasing in v. $\mathbf{c}^\top \mathbf{q}(T)$ is independent of v, and $h(D)$ is decreasing in v. The

next term, $(1-q^D(T-1))\mathbf{g}(v)^\top\mathbf{q}(T) - \mathbf{g}^\top(v)\mathbf{q}(T-1)$, is equal to

$$\begin{aligned}
&(1-q^D(T-1))\mathbf{g}(v)^\top\mathbf{q}(T) - \mathbf{g}^\top(v)\mathbf{q}(T-1)\\
&= (1-q^D(T-1))(q^L(T)-q^L(T-1))h(R^{LPV})\\
&+ (1-q^D(T-1))(q^H(T)-q^H(T-1))h(R^{HPV}).
\end{aligned}$$

according to the definition of the vector $\mathbf{g}(v)$. By the Bellman equation Eq (2.4), both $h(R^{LPV})$ and $h(R^{HPV})$ are negative and decreasing in v. By Assumption 2, $(1-q_n^D(T-1))q_n^L(T) - q_n^L(T-1) \geq 0$, and $(1-q_n^D(T-1))q_n^H(T) - q_n^H(T-1) \geq 0$. Thus, the this term is also decreasing in v. $-q^D(T-1)v$ is also clearly decreasing in v. In sum, we proved that $\tilde{h}(T,v)$ is decreasing in v.

Now, we prove the induction step. Assuming $\tilde{h}(s+1,v)$ is decreasing in v, we want to prove that $\tilde{h}(s,v)$ is also decreasing in v. By the Bellman's equation (2.3a), we have

$$\begin{aligned}
h(s,v) &= -\gamma(v) + \mathbf{c}^\top\mathbf{q}(s)\\
&\quad + \min\big\{\mathbf{g}(v)^\top\mathbf{q}(s) + q^D(s)h(D) + v,\ (1-q^D(s))h(s+1) + q_n^D(s)h_n(D)\big\}\\
&= -\gamma(v) + \mathbf{c}^\top\mathbf{q}(s) + \min\{0, \tilde{h}(s+1)\} + \mathbf{g}(v)^\top\mathbf{q}(s) + q_n^D(s)h_n(D) + v.
\end{aligned}$$

Thus, we have

$$\begin{aligned}
&\tilde{h}(s,v) := (1-q^D(s-1))h(s,v) - \mathbf{g}(v)^\top\mathbf{q}(s-1) - v\\
&= \Big((1-q^D(s-1))\Big(-\gamma(v) + \mathbf{c}^\top\mathbf{q}(s) + \min\{0,\tilde{h}(s+1)\} + \mathbf{g}(v)^\top\mathbf{q}(s) + q^D(s)h(D) + v\Big)\Big)\\
&- \mathbf{g}(v)^\top\mathbf{q}(s-1) - v\\
&= \Big((1-q^D(s-1))\Big(-\gamma(v) + \mathbf{c}^\top\mathbf{q}(s) + \min\{0,\tilde{h}(s+1)\} + q_n^D(s)h_n(D)\Big)\Big)\\
&+ \Big((1-q^D(s-1))\mathbf{g}(v)^\top\mathbf{q}(s) - \mathbf{g}(v)^\top\mathbf{q}(s-1)\Big) - q^D(s-1)v
\end{aligned}$$

We now analyze the monotonicity of each term above.

The first term, $\Big((1-q^D(s-1))\Big(-\gamma(v) + \mathbf{c}^\top\mathbf{q}(s) + \min\{0,\tilde{h}(s+1)\} + q_n^D(s)h_n(D)\Big)\Big)$,

is decreasing in v, since $-\gamma(v)$, $h(D)$, and $\tilde{h}(s+1,v)$ are decreasing in v. The second term, $(1-q^D(s-1))\mathbf{g}(v)^\top\mathbf{q}(s) - \mathbf{g}(v)^\top\mathbf{q}(s-1)$, is equal to

$$\begin{aligned}
&(1-q^D(s-1))\mathbf{g}(v)^\top\mathbf{q}(s) - \mathbf{g}^\top(v)\mathbf{q}(s-1) \\
&= (1-q^D(s-1))(q^L(s)-q^L(s-1))h(R^{LPV}) \\
&+ (1-q^D(s-1))(q^H(s)-q^H(s-1))h(R^{HPV}).
\end{aligned}$$

Recall that $h(R^{LPV})$ and $h(R^{HPV})$ are negative and decreasing in v. By Assumption 2, $(1-q_n^D(s-1))q_n^L(s) - q_n^L(s-1) \geq 0$ and $(1-q_n^D(s-1))q_n^H(s) - q_n^H(s-1) \geq 0$, so the second term is also decreasing in v. $q^D(s-1)v$ is also clearly decreasing in v. Therefore, we conclude that $\tilde{h}(s,v)$ is also decreasing in v. ■

Proof of Theorem 2

Consider the Bellman's equation (2.3), the optimal decision is to inspect if and only if $\tilde{h}_n(s+1,v) = (1-q_n^D(s))h_n(s+1,v) - \mathbf{g}_n(v)^\top\mathbf{q}_n(s) - v$ is positive. The rest is similar to the proof of the Theorem 1. ■

APPENDIX B

DETAILED STEPS OF CHAPTER 2 DATA PROCESSING

We use two data sets of EPA Enforcement and Compliance History Online (ECHO) database: *ICIS_AIR* and the *ECHO Exporter*. These data sets can be downloaded via `https://echo.epa.gov/files/echodownloads/ICIS-AIR_downloads.zip` and `https://echo.epa.gov/files/echodownloads/echo_exporter.zip`, respectively. All our analysis is based on the data download on February 16, 2020.

This is a comprehensive data set that provides information on the facilities, their inspection history, and enforcement actions. We extract and aggregate data across different CSV files. Each facility has two unique identification code: *PGM_SYS_ID* and *REGISTRY_ID*. *ICIS_AIR* csv files are based on *PGM_SYS_ID* and *ECHO Exporter* data is based on *REGISTRY_ID*. *ICIS-AIR_FACILITIES.csv* provides both codes for each facility which helps us to match the data extracted across all the files through one of these codes.

Table B.1 shows the extracted features from each file and their descriptions in detail. As mentioned in §2.5, we filter the data for the major and synthetic minor (SMI) facilities in Region 2. For data resolution, we also filter for the inspections conducted during 2002-2016.

B.1 Facilities Information

We extract the information on facilities attributes from two different files. From *ICIS-AIR_FACILITIES.csv*, we use county name *(COUNTY_NAME)*, type of industry *(NAICS_CODE)*, type of ownership *(FACILITY_TYPE_CODE)*, and air pollutant class code or facility emission size *(AIR_POLLUTANT_CLASS_CODE)*. From *ECHO_EXPORTER.csv* file, we extract non-attainment flag *(FAC_NAA_FLAG)* and environmental justice flag *(EJSCREEN_FLAG_US)*.

B.2 Inspection and Enforcement History

We extract the information on facilities inspection history from the *ICIS-AIR_FCES_PCES.csv* file. We filter the data for on-site inspections conducted through EPA or states. We exclude off-site monitorings as they are done in regulators' offices and require fewer resources. We also do not differentiate between full and partial inspections.

We extract the date of the on-site inspections *(ACTUAL_END_DATE)* for each facility. Facilities' enforcement history is extracted from the *ICIS-AIR_FORMAL_ACTIONS.csv* file. For each enforcement entry, we obtain the date that the settlement has been paid *(SETTLEMENT_ENTERED_DATE)* and the amount of the penalty *(PENALTY_AMOUNT)*. A challenge we faced in the analysis is that the inspection history file *ICIS-AIR_FCES_PCES.csv* does not include the inspection outcomes, i.e., the file does not show which inspection led to enforcement action. *ICIS-AIR_VIOLATION_HISTORY.csv* provides information on a subset of the violations called federally reportable violations (FRV) [22], but it is not a reasonable choice for determining the LPV violations. Firstly because not all the LPVs are federally reportable, and FRVs are only a small portion of all the violations. Secondly, there are other activities rather than on-site inspections which can lead to FRVs, and there is not a clear way that we can differentiate FRVs resulting from on-site inspections from the rest [29].

ICIS-AIR_FCES_PCES.csv also does not label whether an inspection is regular or restoration (follow-ups after a violation is detected). We solve these issues using the approach outlined in in §2.5.1.

B.2.1 Regular Inspections.

We identify *regular inspections* based on the assumption that a regular inspection typically does not occur within a short period of time from the last inspection. We assume this period to be six months. To be specific, for any facility, *regular inspections* are considered the ones that occurred at least six months after their preceding inspection, and when it is not in

violation restoration.

We then classify the outcome of regular inspections as follows. For low priority violations (LPV), we assume a regular inspection leads to a LPV if there is at least one follow-up inspection within six months, and an enforcement action within the 1,000 days of the original inspection. Six months is the period within which the regulator is required to conduct restoration inspections for low priority violations. The 1,000 day window is chosen because we learned that that 90% of the enforcement actions occur within the 1,000 days of the inspections, using a subset in which there is only one inspection and one enforcement action available for a single facility [29].

Fortunately, the events of high priority violations (HPV) are explicitly labeled in the data set. We extract the data on HPVs from *ICIS-AIR_VIOLATION_HISTORY.csv*. For each facility, *HPV_DAYZERO_DATE* column provides the discovery date of the HPVs, which can be within 90 days of the HPV inspection. Matching the inspection dates (*ACTUAL_END_DATE*) extracted from the *ICIS-AIR_FCES_PCES.csv* file with the *HPV_DAYZERO_DATE* that occurred in their 90 days proceeding interval would determine the inspections that resulted in high priority violations [29].

B.2.2 Restoration Inspections.

We define restoration inspections as those that occurred within six months of their preceding LPV inspection or while the facility is in HPV restoration. We use LPV restoration inspections to determine the restoration time of the low priority violations. Note that there might be multiple restoration inspections following a violation; we consider the latest one as the time of the restoration.

The restoration date of HPV inspections are explicitly provided in *HPV_RESOLVED_DATE* of *ICIS-AIR_VIOLATION_HISTORY.csv*. Unlike LPV restoration, HPV restorations can take more than six months.

Table B.1: Data sources.

	File Name	Column Header	Description
Facility information	ICIS-AIR_FACILITIES.csv	PGM_SYS_ID	Facility ID
		REGISTRY_ID	Facility ID
		AIR_POLLUTANT_CLASS_CODE	Facility emission size
		COUNTY_NAME	County name
		NAICS_CODE**	Type of industry
		FACILITY_TYPE_CODE	Type of ownership
	ECHO_EXPORTER.csv	FAC_NAA_FLAG	Non-attainment flag
		EJSCREEN_FLAG_US	Environmental justice flag
Inspection information	ICIS-AIR_FCES_PCES.csv	PGM_SYS_ID	Facility ID
		ACTUAL_END_DATE	Inspection date
		PROGRAMS_CODE	Applicable air programs
Enforcement actions information	ICIS-AIR_FORMAL_ACTIONS.csv	PGM_SYS_ID	Facility ID
		SETTLEMENT_ENTERED_DATE	Date of receiving the settlement
		PENALTY_AMOUNT	Amount of penalty
High priority violations	ICIS-AIR_VIOLATION_HISTORY.csv	PGM_SYS_ID	Facility ID
		HPV_DAYZERO_DATE	HPV discovery date
		HPV_RESOLVED_DATE	Date of restoration from HPV

* For detailed information on the variables of the table see:
`https://echo.epa.gov/tools/data-downloads/icis-air-download-summary#air-program-codes`
** We use the first three digits of the NAICS code. For more information on NAICS code see: `https://www.census.gov/eos/www/naics/`.

REFERENCES

[1] M. A. Al-Zahrani and A. Abo-Monasar, "Urban residential water demand prediction based on artificial neural networks and time series models", *Water Resources Management*, vol. 29, no. 10, pp. 3651–3662, 2015.

[2] S. Alizamir and S.-H. Kim, "Competing to discover compliance violations: Self-inspections and enforcement policies", *History*, 2017.

[3] ArcGIS, *Environmental justice areas viewer*, `https://www.arcgis.com/apps/webappviewer/index.html?id=f31a188de12467691cae93c3339469c`, 2020.

[4] T. W. Archibald, D. Black, and K. D. Glazebrook, "Indexability and index heuristics for a simple class of inventory routing problems", *Operations Research*, vol. 57, no. 2, pp. 314–326, 2009.

[5] T. Ayer, C. Zhang, A. Bonifonte, A. C. Spaulding, and J. Chhatwal, "Prioritizing hepatitis c treatment in us prisons", *Operations Research*, vol. 67, no. 3, pp. 853–873, 2019.

[6] V. Bakker, A. Molderink, J. L. Hurink, and G. J. Smit, "Domestic heat demand prediction using neural networks", in *2008 19th International Conference on Systems Engineering*, IEEE, 2008, pp. 189–194.

[7] H. Bastani, O. Bastani, and C. Kim, "Interpreting predictive models for human-in-the-loop analytics", *arXiv preprint arXiv:1705.08504*, pp. 1–45, 2018.

[8] M. R. Baye, J. Morgan, and P. Scholten, "The value of information in an online consumer electronics market", *Journal of Public Policy & Marketing*, vol. 22, no. 1, pp. 17–25, 2003.

[9] D. P. Bertsekas, *Dynamic Programming and Optimal Control*, 4th. Athena Scientific, 2007, vol. II.

[10] D. Bertsimas and J. Niño-Mora, "Restless bandits, linear programming relaxations, and a primal-dual index heuristic", *Operations Research*, vol. 48, no. 1, pp. 80–90, 2000.

[11] J. R. Birge, J. Drogosz, and I. Duenyas, "Setting single-period optimal capacity levels and prices for substitutable products", *International Journal of Flexible Manufacturing Systems*, vol. 10, no. 4, pp. 407–430, 1998.

[12] G. Bitran and R. Caldentey, "An overview of pricing models for revenue management", *Manufacturing & Service Operations Management*, vol. 5, no. 3, pp. 203–229, 2003.

[13] S. Boriah, V. Chandola, and V. Kumar, "Similarity measures for categorical data: A comparative evaluation", in *Proceedings of the 2008 SIAM international conference on data mining*, SIAM, 2008, pp. 243–254.

[14] F. Caro and J. Gallien, "Dynamic assortment with demand learning for seasonal consumer goods", *Management Science*, vol. 53, no. 2, pp. 276–292, 2007.

[15] F. Caro and J. Gallien, "Clearance pricing optimization for a fast-fashion retailer", *Operations Research*, vol. 60, no. 6, pp. 1404–1422, 2012.

[16] M. Condon, "Citizen scientists, data transparency, and the mining industry", *Natural Resources & Environment*, vol. 32, no. 2, pp. 24–28, 2017.

[17] J. Connor, "A robust neural network filter for electricity demand prediction", *Journal of Forecasting*, vol. 15, no. 6, pp. 437–458, 1996.

[18] S. Deo, S. Iravani, T. Jiang, K. Smilowitz, and S. Samuelson, "Improving health outcomes through better capacity allocation in a community-based chronic care model", *Operations Research*, vol. 61, no. 6, pp. 1277–1294, 2013.

[19] W. Elmaghraby and P. Keskinocak, "Dynamic pricing in the presence of inventory considerations: Research overview, current practices, and future directions", *Management science*, vol. 49, no. 10, pp. 1287–1309, 2003.

[20] EPA, *Evolution of the clean air act*, `https://www.epa.gov/clean-air-act-overview/evolution-clean-air-act`, 2000.

[21] EPA, *Benefits and costs of the clean air act 1990-2020, the second prospective study*, `https://www.epa.gov/clean-air-act-overview/benefits-and-costs-clean-air-act-1990-2020-second-prospective-study`, 2011.

[22] EPA, *Guidance on federally-reportable violations for stationary air sources*, `https://www.epa.gov/sites/production/files/2013-10/documents/caastationary-guidance.pdf`, 2014.

[23] EPA, *Timely and appropriate enforcement response to high priority violations*, `https://www.epa.gov/sites/production/files/2015-01/documents/hpvpolicy2014.pdf`, 2014.

[24] EPA, *Clean air act stationery compliance monitoring strategy*, https://www.epa.gov/sites/production/files/2013-09/documents/cmspolicy.pdf, 2016.

[25] EPA, *Air quality improves as america grows*, https://gispub.epa.gov/air/trendsreport/2019/documentation/AirTrends_Flyer.pdf, 2019.

[26] EPA, *State compliance monitoring expectations*, https://echo.epa.gov/trends/comparative-maps-dashboards/state-compliance-monitoring-expectations, 2019.

[27] EPA, *Clean air act section 112(r): Accidental release prevention and risk management plan rule*, https://www.epa.gov/sites/production/files/2020-03/documents/caa112_rmp_factsheet_march_2020_final.pdf, 2020.

[28] EPA, *Non-attainment areas for criteria pollutants*, https://www.epa.gov/green-book, 2020.

[29] EPA, *Private communication*, 2020.

[30] EPA, *Who has to obtain a title v permit?*, https://www.epa.gov/title-v-operating-permits/who-has-obtain-title-v-permit, 2020.

[31] K. J. Ferreira, B. H. A. Lee, and D. Simchi-Levi, "Analytics for an online retailer: Demand forecasting and price optimization", *Manufacturing & Service Operations Management*, vol. 18, no. 1, pp. 69–88, 2015.

[32] R. Fryer and P. Harms, "Two-armed restless bandits with imperfect information: Stochastic control and indexability", *Mathematics of Operations Research*, vol. 43, no. 2, pp. 399–427, 2017.

[33] P. E. Gill, W. Murray, and M. H. Wright, "Practical optimization", *London: Academic Press, 1981*, 1981.

[34] A. Gillespie, *Foundations of economics*. Oxford University Press, USA, 2014.

[35] K. D. Glazebrook, C. Kirkbride, and J. Ouenniche, "Index policies for the admission control and routing of impatient customers to heterogeneous service stations", *Operations Research*, vol. 57, no. 4, pp. 975–989, 2009.

[36] K. D. Glazebrook, H. Mitchell, and P. Ansell, "Index policies for the maintenance of a collection of machines by a set of repairmen", *European Journal of Operational Research*, vol. 165, no. 1, pp. 267–284, 2005.

[37] K. D. Glazebrook, D. Ruiz-Hernandez, and C. Kirkbride, "Some indexable families of restless bandit problems", *Advances in Applied Probability*, vol. 38, no. 3, pp. 643–672, 2006.

[38] J. C. Gower, "A general coefficient of similarity and some of its properties", *Biometrics*, pp. 857–871, 1971.

[39] D. Graczová and P. Jacko, "Generalized restless bandits and the knapsack problem for perishable inventories", *Operations Research*, vol. 62, no. 3, pp. 696–711, 2014.

[40] T. Hastie, R. Tibshirani, and J. Friedman, *The elements of statistical learning: data mining, inference, and prediction*. Springer Science & Business Media, 2009.

[41] T. Hastie, R. Tibshirani, J. Friedman, and J. Franklin, "The elements of statistical learning: Data mining, inference and prediction", *The Mathematical Intelligencer*, vol. 27, no. 2, pp. 83–85, 2005.

[42] A. K. Jain, J. Mao, and K. M. Mohiuddin, "Artificial neural networks: A tutorial", *Computer*, vol. 29, no. 3, pp. 31–44, 1996.

[43] S.-H. Kim, "Time to come clean? disclosure and inspection policies for green production", *Operations Research*, vol. 63, no. 1, pp. 1–20, 2015.

[44] E. Lee, M. S. Lavieri, and M. Volk, "Optimal screening for hepatocellular carcinoma: A restless bandit model", *Manufacturing & Service Operations Management*, vol. 21, no. 1, pp. 198–212, 2018.

[45] C. Maglaras and J. Meissner, "Dynamic pricing strategies for multiproduct revenue management problems", *Manufacturing & Service Operations Management*, vol. 8, no. 2, pp. 136–148, 2006.

[46] V. Mani and S. Muthulingam, "Does learning from inspections affect environmental performance? Evidence from unconventional well development in Pennsylvania", *Manufacturing & Service Operations Management*, vol. 21, no. 1, pp. 177–197, 2018.

[47] MathWorks, *Find minimum of constrained nonlinear multivariable function*, `https://www.mathworks.com/help/optim/ug/fmincon.html`, 2020.

[48] McKinsey, *Five facts: How customer analytics boosts corporate performance*, `https://www.mckinsey.com/business-functions/marketing-and-sales/our-insights/five-facts-how-customer-analytics-boosts-corporate-performance`, 2014.

[49] McKinsey, *Capturing value from your customer data*, https://www.mckinsey.com/business-functions/mckinsey-analytics/our-insights/capturing-value-from-your-customer-data, 2017.

[50] MIT, *Dissimilarity Matrix Calculation*, http://web.mit.edu/~r/current/arch/i386_linux26/lib/R/library/cluster/html/daisy.html, 2020.

[51] F. J. Mulhern and R. P. Leone, "Implicit price bundling of retail products: A multiproduct approach to maximizing store profitability", *Journal of Marketing*, vol. 55, no. 4, pp. 63–76, 1991.

[52] F. Murtagh and P. Legendre, "Ward's hierarchical agglomerative clustering method: Which algorithms implement ward's criterion?", *Journal of classification*, vol. 31, no. 3, pp. 274–295, 2014.

[53] J. Nino-Mora, "Restless bandits, partial conservation laws and indexability", *Advances in Applied Probability*, vol. 33, no. 1, pp. 76–98, 2001.

[54] S. S. Oren, S. A. Smith, and R. B. Wilson, "Multi-product pricing for electric power", *Energy Economics*, vol. 9, no. 2, pp. 104–114, 1987.

[55] Ö. Özer, O. Ozer, and R. Phillips, *The Oxford handbook of pricing management*. Oxford University Press, 2012.

[56] C. H. Papadimitriou and J. N. Tsitsiklis, "The complexity of optimal queuing network control", *Mathematics of Operations Research*, vol. 24, no. 2, pp. 293–305, 1999.

[57] M. J. Powell, "The convergence of variable metric methods for nonlinearly constrained optimization calculations", in *Nonlinear programming 3*, Elsevier, 1978, pp. 27–63.

[58] M. J. a. Powell, "A fast algorithm for nonlinearly constrained optimization calculations", in *Numerical analysis*, Springer, 1978, pp. 144–157.

[59] D. J. Reibstein and H. Gatignon, "Optimal product line pricing: The influence of elasticities and cross-elasticities", *Journal of marketing research*, vol. 21, no. 3, pp. 259–267, 1984.

[60] P. Rusmevichientong, B. Van Roy, and P. W. Glynn, "A nonparametric approach to multiproduct pricing", *Operations Research*, vol. 54, no. 1, pp. 82–98, 2006.

[61] S. A. Smith and D. D. Achabal, "Clearance pricing and inventory policies for retail chains", *Management Science*, vol. 44, no. 3, pp. 285–300, 1998.

[62] K. T. Talluri and G. J. Van Ryzin, *The theory and practice of revenue management*. Springer Science & Business Media, 2006, vol. 68.

[63] R. L. Thorndike, "Who belongs in the family?", *Psychometrika*, vol. 18, no. 4, pp. 267–276, 1953.

[64] K. Venkatesh, V. Ravi, A. Prinzie, and D. Van den Poel, "Cash demand forecasting in atms by clustering and neural networks", *European Journal of Operational Research*, vol. 232, no. 2, pp. 383–392, 2014.

[65] D. Wang, W. Cao, J. Li, and J. Ye, "Deepsd: Supply-demand prediction for online car-hailing services using deep neural networks", in *2017 IEEE 33rd international conference on data engineering (ICDE)*, IEEE, 2017, pp. 243–254.

[66] S. Wang, P. Sun, and F. de Véricourt, "Inducing environmental disclosures: A dynamic mechanism design approach", *Operations Research*, vol. 64, no. 2, pp. 371–389, 2016.

[67] R. R. Weber and G. Weiss, "On an index policy for restless bandits", *Journal of Applied Probability*, vol. 27, no. 3, pp. 637–648, 1990.

[68] P. Whittle, "Restless bandits: Activity allocation in a changing world", *Journal of applied probability*, vol. 25, no. A, pp. 287–298, 1988.

[69] WHO, *Mortality and burden of disease from ambient air pollution*, `https://www.who.int/gho/phe/outdoor_air_pollution/burden/en/`, 2016.

[70] WKBW, *Citizens' photos are part of evidence to shut tonawanda coke*, `https://www.wkbw.com/news/citizens-photos-are-part-of-evidence-to-close-tonawanda-coke`, 2018.